Czech Technical University in Prague
Faculty of Nuclear Sciences and Physical Engineering

MASTER'S THESIS

Optical Interferometers and Quantum Walks

2009

Václav Potoček

Acknowledgments

I would like to thank my supervisor, prof. Igor Jex, for kind support and help during the creation of this thesis, for providing access to all the important references and checking the factual correctness of the manuscript. I am also grateful to my consultant and colleague, Aurél Gábris, for many insightful discussions and hints on various part of the topic and for numerous stylistical and factual corrections improving the text significantly.

Collaboration with partner scientific groups lead by Erika Andersson (Heriott-Watt University of Edinburgh, UK), Christine Silberhorn (Max Planck Institute for the Science of Light, Erlangen, Germany) and Tamás Kiss (Hungarian Academy of Sciences, Budapest, Hungary) is highly appreciated and I would like to thank all the people who made it possible.

Last but not least, I would like to thank Thomas Brougham, as well as others who have read the manuscript, for helping to proof read the text.

Název práce:
Optické interferometry a kvantové procházky

Autor: Václav Potoček

Obor: Matematické inženýrství

Zaměření: Matematická fyzika

Druh práce: Diplomová práce

Vedoucí práce: Prof. Ing. Igor Jex, DrSc., KF, FJFI, ČVUT

Konzultant práce: Aurél Gábris, PhD, KF, FJFI, ČVUT

Abstrakt: Práce popisuje několik experimentálně realizovatelných konfigurací, které implementují kvantovou náhodnou procházku. Výhodou navrhovaných realizací je využití omezeného počtu lineárních optických elementů. Výsledky teoretického rozboru ukazují překvapivé druhy interference, které by mohly rozšířit možnosti kvantové analogie náhodných procházek za hranice dříve popsaných teorií kvantových náhodných procházek.

Klíčová slova: Interferometry, kvantová optika, kvantové náhodné procházky

Title:
Optical Interferometers and Quantum Walks

Author: Václav Potoček

Abstract: The thesis describes several mutually independent experimentally realizable optical interferometers proposed for implementing a quantum walk. In contrast to other realizations, the advantage of the presented implementations is the use of a limited number of linear optics elements. The results of the theoretical study of these devices show various means of interference, which could extend the possibilities of quantum analogy to random walk theory beyond the current quantum walk understanding.

Key words: Interferometers, Quantum optics, Quantum walks

Contents

List of used symbols

The following list covers some of the mathematical symbols and conventions used in the work without prior definition.

Symbol	**Explanation**
$\mathbb{N}$	the set of positive integers, i.e., $\{1, 2, 3, \ldots\}$
$\mathbb{N}_0$	the set of nonnegative integers, i.e., $\{0, 1, 2, 3, \ldots\}$
$\mathbb{Z}$	the set of all integers, i.e., $\{0, 1, -1, 2, -2, \ldots\}$
$\mathbb{R}$	the set of real numbers
$\mathbb{C}$	the set of complex numbers
$\mathbb{1}$	identity operator, identity matrix
α^*	complex conjugate of a complex number α
$A^\dagger$	Hermitian adjoint of an operator A
$\operatorname{Tr} A$	trace of an operator A
$\otimes$	tensor product of operators, vectors or vector spaces
$\Re\alpha$	the real part of a complex number α
$\Im\alpha$	the imaginary part of a complex number α
$n!!$	the double factorial of n: $n(n-2)(n-4)\ldots$; $(-1)!! = 0!! = 1$.
$[x]$	nearest integer to a real number x
$\lfloor x \rfloor$	the integer part, the largest integer not greater than $x \in \mathbb{R}$
(a, b)	an open interval from a to b
$\langle a, b \rangle$	a closed interval from a to b
$f = O(g)$	$\lvert f(x) \rvert$ is bounded above by const. $\times\, g(x)$ asymptotically
$f = \Omega(g)$	$\lvert f(x) \rvert$ is bounded below by const. $\times\, g(x)$ asymptotically
$f = \Theta(g)$	$f(x)$ is bounded both above and below by const. $\times\, g(x)$ asymptotically

Introduction

Quantum walks are an interesting analogue of classical random walks, defined in the framework of quantum mechanics. Many kinds of quantum walks have been studied and several quantum algorithms are based on them. An experimental realization of a quantum walk could also open a way to implement these algorithms. Despite the number of experimental scenarios that have been proposed to implement a quantum walk, e.g., [1,2], only a few actual experimental demonstrations have been published so far—the first evidence is dated 2003 [3]. This thesis describes three new different experimentally realizable configurations which display the behaviour of quantum walks and thus could be used to achieve this goal. One of the algorithms is the subject of a current experiment [4].

The work is organized as follows. In Chapter 1, we provide a brief overview of quantum walks and optical interferometers in general. In Chapter 2, we study the features of a simple interferometer composed of beam splitters and mirrors only. When short light pulses or single photons are inserted, a quantum walk behaviour can be observed in the output arm. In Chapter 3, a more elaborate interferometer is studied where light polarization is used to find a close correspondence to a quantum walk on a line studied by the pioneering works. In Chapter 4, the possibility of using an optical grating as a linear optics element is presented and a third quantum walk experiment is proposed. Finally, we conclude our results.

The main idea of the first two proposed implementations is to use one closed interferometric loop for an arbitrary number of the walk steps, as opposed to more straightforward linear optics implementations, whose space requirements scale quadratically with the number of steps to be performed [2]. Also, the experiment described in Chapter 2 shows a completely new form of a quantum walk sharing many properties with a classical random walk.

We emphasize that the optical interferometers described in Chapters 2, 3 and 4 were not designed by the author. The first studied experimental configuration is a result of collaboration with Erika Andersson, Aurél Gábris, Igor Jex, Tamás Kiss and others, the configuration introduced in Chapter 3 is actually a description of an existing experiment realized by the group of Andreas Schreiber, Katiuscia Cassemiro and Christine Silberhorn. The idea of using diffraction gratings to implement quantum walks comes from Igor Jex and his colleague, Goce Chadzitaskos. The aim of this thesis is to develop a theoretical background for these configurations and to show the connections between them. The mathematical models and their explicit solutions are original.

Chapter 1
Overview of the topic

Let us introduce the most important concepts which will be used in the chapters to follow. In this chapter, we will review the concepts of quantum walks and optical interferometers.

1.1 Quantum walks, basic types and properties

The idea of finding a quantum counterpart of a random walk was first introduced in [5] in 1993. The authors of the mentioned paper studied the behaviour of a one-dimensional spin-$\frac{1}{2}$ particle whose dynamics was determined by a specially defined evolution operator which shifted the particle to the right or to the left depending on its spin state. After every step, a measurement of position was done, collapsing the wave function and bringing randomness into the the time evolution.

Since that work, many authors have introduced other models that shared the idea of "quantum walks". The theory has branched in several ways which are only loosely connected. The main idea extending the first example, which was rather classical, was to drop the intermediate measurements: we let the system evolve freely for some given time and make only one measurement at the end of this interval.

The direct result of this approach is a *discrete time quantum walk with a coin* [6,7,8], which is formulated algebraically as follows. Let $\mathcal{H}_S$ be a discretized position space, where the allowed localized positions of the particle form an orthonormal basis whose vectors are denoted by integer numbers. Let this space be augmented by a two-dimensional "coin space" $\mathcal{H}_C$, which takes the role of the spin space of the original system. Let us define two orthonormal basis states in $\mathcal{H}_C$, denoted $|L\rangle$ and $|R\rangle$. An orthonormal basis of the composed system, whose state space is a tensor product $\mathcal{H}_S \otimes \mathcal{H}_C$, can be found as

$$\{|x,d\rangle = |x\rangle \otimes |d\rangle \mid x \in \mathbb{Z}, d \in \{L,R\}\}. \tag{1.1}$$

The quantum walk is obtained by initializing the system in a state

$$|\psi_i\rangle = |0\rangle \otimes |z\rangle, \tag{1.2}$$

where $|z\rangle \in \mathcal{H}_C$ denotes the initial coin state (or initial *chirality*), and letting it evolve for a given number of discrete time steps. One step then consists of "tossing the coin" and then taking a conditional step of size ± 1 in the position space. Mathematically speaking, the propagator corresponding to one time step is composed of a unitary *coin operator* C, acting on the coin space only, followed by a *step operator* S:

$$U = S \cdot C, \tag{1.3 a}$$

where

$$C = \mathbb{1} \otimes C_0,$$

$$S = \sum_{x \in \mathbb{Z}} \left(|x+1, R\rangle\langle x, R| + |x-1, L\rangle\langle x, L| \right). \tag{1.3 b}$$

As C_0 acts on the previous coin state, there is a strong correlation between the subsequent steps, resulting in a highly non-classic behaviour of the quantum walk.

Making the final measurement on the position space, we can construct a discrete probability distribution of the possible positions where the walker will be found. The distribution of a quantum walk is generally bordered by two sharp peaks which asymptotically move at a linear speed away from the origin, as opposed to a classical random walk, for which the probability distribution is binomial. In relation to this behaviour, the standard deviation of the quantum walk is asymptotically linear in the iteration count as opposed to the classical random walk where it scales with the square root of time. More details about the distribution can be found in [6].

The coin plays a fundamental role in a discrete time quantum walk. As an example, the general properties of a particular quantum walk, such as symmetry of the motion to the left or right, are determined not only by the coin operator C_0 but also depend strongly on the initial coin state $|z\rangle$. The necessity of using the coin space follows from the so-called No-Go Lemma [9], which states that the basic properties expectable from a random walk, combined with the demand of unitary time evolution, restrict a coinless quantum walk on $\mathcal{H}_S$ to a trivial form where each step is taken in the same direction.

As a first possible generalization of this discrete time quantum walk model, we can replace the line by a more complicated graph on which the walker can move. Quantum walks on a circle [6], grids with cyclic boundary conditions [10] or hypercubes [11] were described and even attempts to find some result for general graphs were made [12]. As long as the graph is regular, i.e., has the same number of edges originating from each vertex, it can be treated analogously to the above case of a line, the main difference is that the dimension of the coin space must be altered to allow steps in more directions. The extension to irregular graphs is much more complicated.

Another generalization of the discrete time quantum walk is obtained when we allow position dependence of the coin transformation. The coin operator then becomes a quantum gate controlled by the position space. On a line, for example, a position-dependent coin operator can be written as

$$C = \sum_{x \in \mathbb{Z}} |x\rangle\langle x| \otimes C_x, \tag{1.4}$$

where C_x is a unitary operator on $\mathcal{H}_C$ for each $x \in \mathbb{Z}$. Position-dependent coins arise most often in quantum walk-based search algorithms [10,13] or as one approach to define a discrete time quantum walk on irregular graphs [8]. Also, a quantum walk on a graph with high symmetry degree can be simplified to a walk on a much simpler graph under some conditions [13], possibly inducing a position dependence of the coin on the reduced graph.

In contrast to the discrete time quantum walk model, another way to define a quantum walk follows the idea of a continuous time Markov processes. In a *continuous time quantum walk* on

a graph [8,14,15], one defines a Hamiltonian over the position space $\mathcal{H}_S$ using the adjacency matrix of the graph. The system then evolves according to the Schrödinger equation for a given time, after which a measurement is made. A particular feature of continuous time quantum walks is that no coin space is needed.

The relation of discrete time and continuous time models is nontrivial: these two approaches show very similar results in some areas whereas there are significant differences in other cases [8]. Only very recent articles [16,17] claim to have found some exact correspondences between the two models.

In the whole scope of this work, we will use the term "quantum walks" to refer to discrete time quantum walks on a line.

1.2 Optical interferometers

The main part of the work will be concerned with the action of specially designed *optical interferometers*. Generally, an optical interferometer, or just *interferometer* for short, is a device in which a light beam or pulse coming from a single source is split using a beam splitter to take two or more possible *optical paths* [18]. Using further beam splitters, mirrors and possibly other linear optics elements, the partial wave packets are later directed to the same interferometer arm and the contributions from various paths interfere. Due to the differences in the optical path lengths corresponding to individual paths, and to phase shifts induced by reflections, the wave packets meet with different phase and the interference can be constructive as well as destructive.

An interferometer has an *input arm*, where the light source is directed to, and one or more *output arms*. There may be other available input modes which are not used—generally, it follows from quantum optics that the numbers of input and output modes must be equal. In order to study the interference, one places optical *detectors* to measure the light properties, e.g., intensity, in the output arms. A wide spectrum of optical detectors is also available for measuring the quantum properties of light [19].

The quality of the interference depends mainly on the stability of the interferometer elements but also on the magnitude of the optical path difference. If it is much larger than the *coherence length* of the source light, the interference does not occur. After a quantization of the electromagnetic field is done, this phenomenon is explained by the fact that in a linear medium, there are almost no interactions between distinct photons, so that every photon contributes to the interference output on its own. We can imagine a single photon as a wave packet propagating along the interferometer arms. This wave packet can be split and recombined on the beam splitters. However, if the optical path difference of two interferometer paths is much larger than the mean width of this wave packet, the partial wave packets will have zero overlap and no interference will take place.

We will keep the wave packet picture it in the following text. Especially, we will use the same description for a single photon as for a nonrelativistic particle and define wave functions which can be linear combinations of states corresponding to the wave packets. We will assume that there is an equation of motion for these wave packets, however, we will never need its direct form. We note that wave packets are treated correctly in quantum optics as simultaneous excitations of a large number of optical modes [20] and share the properties we need.

Chapter 2
Quantum walk with a simple delay loop

The first configuration to be studied is based on the principle of a delay loop. It is depicted in Fig. 1. It works as follows: a short coherent unpolarized light pulse is sent into the input arm and gets split on the beam splitter A into the middle and lower arm, denoted M and L. Due to their different optical lengths, the two wavefronts arrive at the beam splitter B at different times. A part of both pulses is then separated into the output arm and measured in the detector, the rest travels through the upper arm U back to the beam splitter A. Due to the geometrical arrangement, the process can in principle repeat an arbitrary number of times.

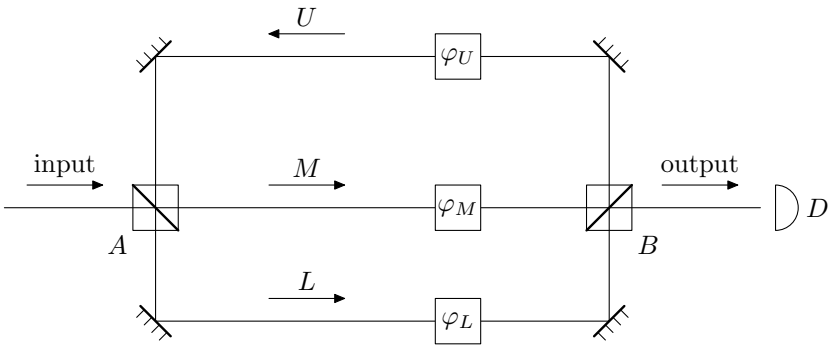

Fig. 1: The first configuration. A and B are both classic beam splitters, D denotes a detector. The interferometer arms can be realized in optical fibre, in which case there is no need for mirrors.

Let the time needed for a light pulse to travel the arms U, M and L be denoted by t_U, t_M and t_L, respectively. In the following, we will always assume that $t_M \neq t_L$ and, where it is important, also that

$$t_L > t_M. \tag{2.1}$$

The time it takes for a pulse to travel through beam splitters, mirrors and phase shifters in the arms is negligible compared to characteristic values of the times t_U, t_M, t_L times (these delays are all in the order of one wavelength whereas t_U, t_M or t_L are about 6 orders of magnitude larger in a typical realization[1]). Let us further denote by t_p the mean duration of the pulse.

If $t_L - t_M \gg t_p$, no interference takes place at the first pass through the beam splitter B as the two parts of the pulse arrive temporally separated. However, if we study the situation after one or more cycles through the upper arm, it can happen that two parts of the pulse which were separated obtain another time difference which causes them to meet again. In this case, we can observe interference.

[1] Values used for this estimate were: wavelength $\lambda \sim 800\,\mathrm{nm}$, optical lengths $l \sim 1\,\mathrm{m}$.

2.1 The interfering optical paths

The condition of interference is that the wavefronts of two or more pulses taking different paths meet at the same point and at the same time (up to the duration of the pulse, t_p), going the same direction. The latter is always met in our configuration: as seen from Fig. 1, each arm has only one direction allowed by the geometric layout. From the superposition principle, it follows that we can postpone the computation of the interference till the point where the pulse is measured, as if the interference took place no sooner.

Therefore, all possible optical paths through the interferometer, starting simultaneously at the input arm and ending at the output arm, will split into infinitely many subsets by their *escape time*. Only the paths within the same subset will interfere.

When looking for optical paths which take *exactly* the same time, we note that the time needed to travel any path from the input to the output is determined only by the number of passes through the lower, middle and upper arm, which we will denote by n_L, n_M and n_U, respectively: the time is

$$t = n_M t_M + n_L t_L + n_U t_U, \tag{2.2}$$

regardless of the order in which the arms are taken. Therefore, two or more paths differing only in this order will each give a different "history" which must be considered one term in the interference.

We will create a simple means of description of the optical paths by words composed of letters U, M and L, written from the left to the right in the order the particular arms are taken. In this formalism, an example of two interfering paths, ending at beam splitter B, can be MUL and LUM.

The geometric arrangement puts some restrictions on such words. First, in order to describe a complete path from the input to the output arm, both its first and last letters can only be M or L. Every M or L except for the last one must be followed by a U and every U again by M or L. This is illustrated diagrammatically in Fig. 2.

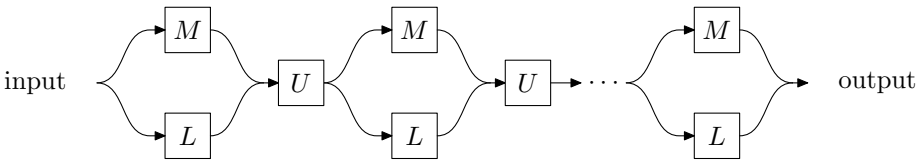

Fig. 2: The rules for the word description of possible optical paths through the delay loop.

It can be seen that one does not lose any information by dropping all the letters U. This gives the *reduced form* of the given word, which can be any sequence of letters M and L. We can reconstruct the full word by replacing $M \mapsto MU$ and $L \mapsto LU$ and erasing the last U formed in this way. For this reason, we will use only the reduced form in the following text.

As a consequence, we can notice the following equation putting a constraint on the numbers of the available letters: $n_U = n_M + n_L - 1$. Plugging this into Eq. (2.2), we can simplify the expression to

$$t = n_M t'_M + n_L t'_L - t_U, \tag{2.3}$$

where

$$t'_M = t_M + t_U \quad \text{and} \quad t'_L = t_L + t_U. \tag{2.4}$$

2.2 Correspondence to a random walk

For some choices of t_M, t_L and t_U, it is possible that not only the paths whose words are permutations of each other will interfere. A sufficient condition for interference is that the times given for the two paths by Eq. (2.3) are closer than t_p. Especially, if the ratio $t'_M : t'_L$ is a rational number, there are paths which take exactly the same time despite they have different n_M and n_L. Namely, if

$$\frac{t'_M}{t'_L} = \frac{p}{q}, \tag{2.5 a}$$

then

$$qt'_M = pt'_L \tag{2.5 b}$$

which implies that the mapping Eq. (2.3) is not injective—it gives the same value of t when we decrease n_M by q and increase n_L by p or *vice versa*. Note that such operation always changes the length of the word, $n_M + n_L$, as $p \neq q$. If $t'_L - t'_M \gg t_p$, two paths whose words have the same length but different n_M and n_L can not interfere as the difference of their times is an integer multiple of $t'_L - t'_M$ or, equivalently, $t_L - t_M$.

The problem of irregularly coinciding escape times can be solved easily by choosing the times t'_M and t'_L themselves much larger than their difference. (On the other hand, however, we are limited by the condition of global coherence.) This creates a carrier pattern in the time domain: escape times of paths with the same $n_M + n_L$ will be grouped together and separated in a finer way by their $n_M : n_L$ ratio. The result is shown in Fig. 3.

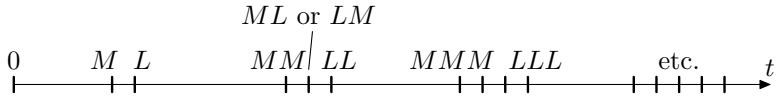

Fig. 3: The possible escape times of the pulse. A combination of letters is used to represent the time marks through Eq. (2.3). Only some marks are labeled. Between MMM and LLL, for example, there are other combinations of three letters in the order of increasing count of L letters.

This leads us to re-parametrizing the escape time by two new variables,

$$\begin{aligned} n &= n_L + n_M, \\ k &= n_L - n_M. \end{aligned} \tag{2.6}$$

The former is the word length and can be used to index the groups created by the proximity of t'_M and t'_L. All paths described by words of a given length will have their escape time in the same group. The latter parameter then numbers the marks in the range of one such group.

Note that for each n, k is bounded between $-n$ and n and has the same parity as n. Under the assumption (2.1), the marks on the time axis will follow a lexicographic ordering of the respective (n,k) couples until the borders of two adjacent groups meet. This happens when

$$\begin{aligned} nt'_L - t_U &\geq (n+1)t'_M - t_U \\ n(t'_L - t'_M) &\geq t'_M \\ n &\geq \frac{t'_M}{t'_L - t'_M}, \end{aligned} \tag{2.7}$$

which puts an upper bound on the number of clearly distinguishable loops.

The correspondence of the system's behaviour with a random walk on a line is straightforward if we call n the iteration count and k the position on a thought line. We can compare taking the middle or lower arm to a step left or right, respectively. Note that all iterations of the walk are observed simultaneously in a single run of the described experiment: they are mapped to a single time line by the $\mathbb{N}_0 \times \mathbb{N}_0 \to \mathbb{R}$ mapping provided by Eq. (2.3). By measuring the escape probability for all the marks in a single group, we can call this a distribution over the possible positions on the line after the given number of steps (see also Sec. 2.6). Finally, recall that after n steps of a random walk, there are exactly the same constraints for k as we found above.

2.3 The quantum mechanical model

Besides the pulse regime described above, the interferometer can also be operated in a single photon mode. In this approach, instead of measuring the intensity of the output signal at the possible escape times, one would insert single photons into the interferometer and measure the distribution of the time instants they are detected at the output. By performing a sufficient number of runs of the experiment, one would use this probability distribution instead of the signal from the intensity detector. In Sec. 2.9, we will prove the exact physical correspondence of these two approaches.

In order to explain single photon phenomena, our mathematical model of the system must be based on quantum mechanical treatment of light instead of classical wave optics. To help with the mathematical description, let us solve the single photon operation first. The simplification obtained in this way is that we can describe the system using one-particle quantum mechanics. After the time evolution is solved, we will rewrite the obtained results in terms of the creation and annihilation field operators, allowing us to consider multi-photon input states, in Sec. 2.9.

The Hilbert space used in the following will be the space of L^2-integrable functions defined on the graph of the interferometer and its vectors wave functions of the photon. We will not work with these wave functions directly, rather, we will define several significant states and study the overlap of the system state with them. These states, as well as the initial state of the incoming photon, will be constructed as minimum uncertainty wave packets described by their mean position. The direction is given by the physical arrangement and the speed is constant.

Because of the detection process, the time evolution of the system is not unitary. However, we can define an *output state* $|\psi_o\rangle$ right at the beginning of the output arm—the amplitude of this state will be equal to the amplitude of probability of detecting the photon after a fixed amount of time. If the photon is not detected, this part of the wave function is lost, leaving only the part supported by the inner parts of the interferometer. There is no need to renormalize the wave function after such a projection—this way we can reflect the fact that the subsequent results are actually conditional probabilities with no extra work.

There is an alternative approach possible: if we replace the detector by an half-infinite line never coming back to the interferometer, the parts of the wave function overlapping $|\psi_o\rangle$ will continue travelling along this line, effectively projected out of the picture. The advantage is that if we do a similar replacement of the input arm, we will recover the unitary nature of the time evolution. This approach justifies the usage of a propagator to describe the system's time evolution.

Let us further describe the action of a beam splitter on the example of the beam splitter A in our layout. It has two input and two output modes. As indicated above, we will model these using two plus two wave packets labelled by the arms they are lying on. These states are shown in Fig. 4.

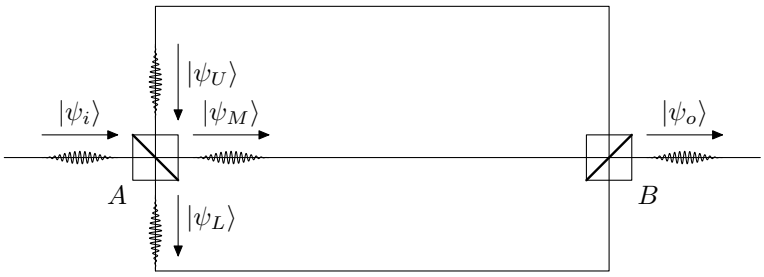

Fig. 4: The selected photon states used for the mathematical description. Both the length of the pulses and their distance from the beam splitters are highly magnified.

If a photon arrives at the beam splitter in a general linear combination of the two input states, $\alpha|\psi_i\rangle + \beta|\psi_U\rangle$, after a certain time of interaction, its state is transformed into a linear combination of the two output states, $\gamma|\psi_M\rangle + \delta|\psi_U\rangle$, by the rule

$$\begin{pmatrix} \gamma \\ \delta \end{pmatrix} = \begin{pmatrix} t_A & -r_A^* \\ r_A & t_A^* \end{pmatrix} \begin{pmatrix} \alpha \\ \beta \end{pmatrix} = \mathcal{R}_A \begin{pmatrix} \alpha \\ \beta \end{pmatrix}. \tag{2.8}$$

Here we assume that A is an ideal passive linear beam splitter.

Alternatively, we could write

$$\begin{aligned} |\psi_i\rangle &\mapsto t_A|\psi_M\rangle + r_A|\psi_L\rangle, \\ |\psi_U\rangle &\mapsto t_A^*|\psi_L\rangle - r_A^*|\psi_M\rangle. \end{aligned} \tag{2.9}$$

The index A denotes the beam splitter we are describing. See also App. A for operator description of this action.

The parameters t_A and r_A are two complex numbers called *transmission* and *reflection amplitudes*, respectively. They must satisfy the condition

$$|t_A|^2 + |r_A|^2 = 1 \tag{2.10}$$

for the matrix $\mathcal{R}_A$ to be unitary, otherwise they are arbitrary. (The condition on unitarity restricts the elements of $\mathcal{R}_A$ to two complex degrees of freedom plus a global phase, which is ignored here.) The location of minus signs and complex conjugates in $\mathcal{R}_A$ is merely a convention, another choice would be balanced by change of phases of t_A and r_A.

In the beam splitter A, we have chosen the input mode out of the interferometer input to be preferred by not obtaining any complex conjugates in Eq. (2.9). Similarly, we will choose the left hand side input mode of the beam splitter B for the same.

Usually, one also defines

$$T_A = |t_A|^2 \quad \text{and} \quad R_A = |r_A|^2 \tag{2.11}$$

called the *transmittance* and *reflectivity* of the beam splitter. These parameters are independent of the phases of t_A and r_A and thus provide an incomplete description of the beam splitter, however, they have a direct interpretation familiar from classical optics. The condition (2.10) can be rewritten as

$$T_A + R_A = 1. \tag{2.12}$$

For the free travel along the interferometer arms, we can define a reference wave packet on both ends of each arm ($|\psi_{a1}\rangle$, $|\psi_{a2}\rangle$), these two being related by a spatial shift. A photon needs some time t_a to travel the length of the arm. Similarly to a beam splitter, we will describe this time evolution by a propagator, specifically by the matrix element $\langle\psi_{a2}|U(t_a)|\psi_{a1}\rangle$. This reduces to some unit complex number, $e^{i\varphi}$. The phase φ will include the phase difference caused by the elapsed time t_a, any possible artificial phase shift put on the arm and possibly some other phase shifts neglected elsewhere. This way, we will define and use the total phase shifts φ_M, φ_L and φ_U, corresponding to the middle, lower and upper arms, respectively.

2.4 The path sum

Instead of computing the state of the system after some fixed time, we will aim to find an expression for the matrix element

$$\alpha(t) = \langle\psi_o|U(t)|\psi_i\rangle \tag{2.13}$$

directly. This amplitude gives the escape probability after time t by the formula

$$P(t) = |\alpha(t)|^2. \tag{2.14}$$

After the first action of beam splitter A, the state is a linear combination of $|\psi_M\rangle$ and $|\psi_L\rangle$. Thus, we can use a decomposition of unity to obtain

$$U_A|\psi_i\rangle = P_M U_A|\psi_i\rangle + P_L U_A|\psi_i\rangle \tag{2.15}$$

where P_M and P_L are orthogonal projectors on the one-dimensional subspaces spanned by $|\psi_M\rangle$ and $|\psi_L\rangle$, respectively. Now if $t > t'_L$, the photon must take the upper arm, passing through the state $|\psi_U\rangle$. However, after the action of both of the projectors in Eq. (2.15), the first time to reach nonzero overlap with this state is uniquely given:

$$\begin{aligned}\langle\psi_o|U(t)|\psi_i\rangle &= \langle\psi_o|U(t-t'_M)P_U U(t'_M - t_A)P_M U_A|\psi_i\rangle + \\ &\quad + \langle\psi_o|U(t-t'_L)P_U U(t'_L - t_A)P_L U_A|\psi_i\rangle = \\ &= \langle\psi_o|U(t-t'_M)|\psi_U\rangle\langle\psi_U|U(t'_M - t_A)P_M U_A|\psi_i\rangle + \\ &\quad + \langle\psi_o|U(t-t'_L)|\psi_U\rangle\langle\psi_U|U(t'_L - t_A)P_L U_A|\psi_i\rangle.\end{aligned} \tag{2.16}$$

From this equation, we can see that the problem of determining $\alpha(t)$ was transformed to computing several matrix elements of evolution operators on shorter time intervals. In both terms of the sum, there is one matrix element with an initial state of $|\psi_U\rangle$ and time t shortened by t'_M or t'_L,

and one matrix element corresponding to taking the middle or the lower path, respectively. We will call the latter an *irreducible* matrix element.

When computing the elements with initial state of $|\psi_U\rangle$, we note that we can deal with it exactly the same way as we did above with $|\psi_i\rangle$, so the subscript can be simply substituted in all the above formulas.

In this way we can reduce the time t down to some remainder t_r, leaving the last element of $\langle\psi_o|U(t_r)|\psi_U\rangle$. This element is both irreducible and nonzero only if $t_r = t_M$ or $t_r = t_L$. Due to the algebraic independence of t'_M and t'_L, this condition filters out all elements of the exponentially growing sum except for those representing the possible optical paths from the input arm to the output arm, taking exactly the time t. (See Fig. 5 for an example of all the optical paths taking a given time.) For this reason, we will call this sum a *path sum*. This concept is in fact a discretized case of *path integral* and its usability for describing quantum random walks has been well-known before, see e.g. [6].

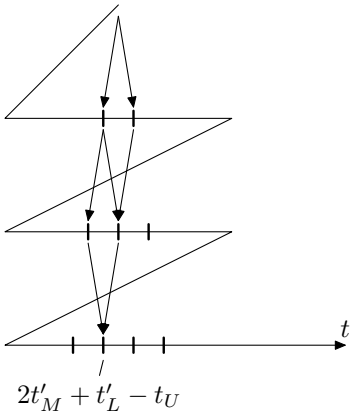

Fig. 5: An illustration of all the optical paths ending at the same escape time of $2t'_M + t'_L - t_U$. The time line is broken to show the artificial partitioning into random walk iterations. Marking the instants the photon passes the beam splitter B, we can note three possible ways to the chosen mark. From the leftmost one to the rightmost one, these are called MML, MLM and LMM in our terminology.

As defined in Sec. 2.1, each optical path is described by a word W composed of letters M and L. For each word containing the letter M n_M times and the letter L n_L times, there will be exactly one product of the irreducible matrix elements:

- $\langle\psi_U|U(t'_\ell - t_A)P_\ell U_A|\psi_i\rangle$, where ℓ is the first letter of W,
- $\langle\psi_U|U(t'_\ell - t_A)P_\ell U_A|\psi_U\rangle$ for every letter ℓ between the first and the last one,
- $\langle\psi_o|U(t_\ell)|\psi_U\rangle$, where ℓ is the last letter of W.

Note that if W has only one letter, ℓ, there is just one term, $\langle\psi_o|U(t_\ell)|\psi_i\rangle$.

We will find explicit forms for all these possible irreducible matrix elements. Starting with the first one,

$$\begin{aligned} U_A|\psi_i\rangle &= t_A|\psi_M\rangle + r_A|\psi_L\rangle \\ P_M U_A|\psi_i\rangle &= t_A|\psi_M\rangle \\ P_L U_A|\psi_i\rangle &= r_A|\psi_L\rangle \end{aligned} \tag{2.17}$$

In both cases, this is a basis state multiplied by some single matrix element of U_A. Now we could define an analogous orthogonal system near the beam splitter B. We would then split $U(t'_\ell - t_A)$ to the free time evolution along the particular arm, the action of the beam splitter B (filtering the output to the upper arm) and the free evolution by time $t_U - t_B$ along the upper arm. The procedure is straightforward, so let us give just the result directly:

$$\begin{aligned}\langle\psi_U|U(t_M - t_A)P_M U_A|\psi_i\rangle &= t_A e^{i\varphi_M} r_B e^{i\varphi_U} = e^{i(\varphi_M+\varphi_U)} t_A r_B \\ \langle\psi_U|U(t_L - t_A)P_L U_A|\psi_i\rangle &= r_A e^{i\varphi_L} t_B^* e^{i\varphi_U} = e^{i(\varphi_L+\varphi_U)} r_A t_B^*.\end{aligned} \tag{2.18}$$

All the other irreducible matrix elements can be expressed similarly:

$$\begin{aligned}\langle\psi_U|U(t'_M - t_A)P_M U_A|\psi_U\rangle &= -e^{i(\varphi_M+\varphi_U)} r_A^* r_B \\ \langle\psi_U|U(t'_L - t_A)P_L U_A|\psi_U\rangle &= e^{i(\varphi_L+\varphi_U)} t_A^* t_B^* \\ \langle\psi_o|U(t_M)|\psi_U\rangle &= -e^{i\varphi_M} r_A^* t_B \\ \langle\psi_o|U(t_L)|\psi_U\rangle &= -e^{i\varphi_L} t_A^* r_B^* \\ \alpha(t_M) = \langle\psi_o|U(t_M)|\psi_i\rangle &= e^{i\varphi_M} t_A t_B \\ \alpha(t_L) = \langle\psi_o|U(t_L)|\psi_i\rangle &= -e^{i\varphi_L} r_A r_B^*\end{aligned} \tag{2.19}$$

This in fact allows us to find a closed form for $\alpha(t)$ for t given by Eq. (2.3). However, it is necessary to separate the case $n = 1$ as shown above and make some general observations starting from $n = 2$. So, for computing $\alpha(n_M t'_M + n_L t'_L - t_U)$, which we can denote for simplicity $\alpha(n_M, n_L)$, we need to sum the above product over all words W composed of n_M times the letter M and n_L times the letter L. These words split into four groups depending on their first and last letter. Due to the construction above, we can see that all the words in one group will contribute in the sum by the same term, so only the cardinality of each of these four subsets is needed.

Using the notation that the binomial coefficients outside the Pascal's triangle are zero, there are $\binom{n-2}{n_L}$ words both beginning and ending by M, $\binom{n-2}{n_M}$ words both beginning and ending by L and $\binom{n-1}{n_M-1}$ for both the remaining cases. Thus the general form of the sum $\alpha(n_M, n_L)$ is

$$\begin{aligned}\alpha(n_M, n_L) = e^{i\varphi(n_M,n_L)} \Bigg(&\binom{n-2}{n_L} (t_A r_B)(-r_A^* t_B)(-r_A^* r_B)^{n_M-2} (t_A^* t_B^*)^{n_L} + \\ &+ \binom{n-2}{n_M} (r_A t_B^*)(-t_A^* r_B^*)(-r_A^* r_B)^{n_M} (t_A^* t_B^*)^{n_L-2} + \\ &+ \binom{n-2}{n_M-1} \left((t_A r_B)(-t_A^* r_B^*) + (r_A t_B^*)(-r_A^* t_B)\right) (-r_A^* r_B)^{n_M-1} (t_A^* t_B^*)^{n_L-1} \Bigg)\end{aligned} \tag{2.20}$$

where the phase

$$\varphi(n_M, n_L) = n_M\varphi_M + n_L\varphi_L + (n-1)\varphi_U$$

can be found to be exactly the same in all terms. Noticing other common terms, this formula can be subsequently significantly simplified to

$$\begin{aligned}\alpha(n_M, n_L) = e^{i\varphi(n_M,n_L)} &(-r_A^* r_B)^{n_M-1} (t_A^* t_B^*)^{n_L-1} \times \\ &\times \left(\binom{n-2}{n_L} T_A T_B + \binom{n-2}{n_M} R_A R_B - \binom{n-2}{n_M-1} (T_A R_B + R_A T_B) \right),\end{aligned} \tag{2.21}$$

where we reused the symbols defined in Eq. (2.11).

Using the relation

$$T_A R_B + R_A T_B = T_A(1-T_B)+R_A(1-R_B) = T_A+R_A-T_AT_B-R_AR_B = 1-T_AT_B-R_AR_B, \quad (2.22)$$

we can use Pascal's rule to simplify Eq. (2.21) even further to

$$\begin{aligned}\alpha(n_M,n_L) = e^{i\varphi(n_M,n_L)}(-r_A^* r_B)^{n_M-1}(t_A^* t_B^*)^{n_L-1}\times \\ \times\left(\binom{n-1}{n_L}T_AT_B + \binom{n-1}{n_M}R_AR_B - \binom{n-2}{n_M-1}\right).\end{aligned} \quad (2.23)$$

The special cases (corresponding to the direct pass through the interferometer), collected in Eq. (2.19),

$$\begin{aligned}\alpha(1,0) = \alpha(t_M) = e^{i\varphi_M}t_At_B, \\ \alpha(0,1) = \alpha(t_L) = e^{i\varphi_L}(-r_Ar_B^*),\end{aligned} \quad (2.24)$$

must be excluded from Eq. (2.23) unless we define the binomial coefficients $\binom{-1}{k}$ to be zero for all k. However, we will avoid this since such a definition would break the Pascal's rule.

2.5 The recurrence relation

Let us relate the behaviour of the interferometer to a random walk by finding a suitable recurrence relation. Denoting by $P_{n,k}$ the probability of finding the walker on the position k after n steps, a classical random walk is governed by the relation

$$P_{n,k} = p_L P_{n-1,k+1} + p_R P_{n-1,k-1}, \quad (2.25)$$

where p_L and p_R are the probabilities of taking a step to the left or to the right, respectively. It is also important to state an initial condition which is usually chosen to be $P_{0,0} = 1$.

Studying Eq. (2.23), we observe that Pascal's rule implies

$$\begin{aligned}\alpha(n_M,n_L) = e^{i\varphi(n_M,n_L)-i\varphi(n_M-1,n_L)}(-r_A^*r_B)\alpha(n_M-1,n_L)+ \\ + e^{i\varphi(n_M,n_L)-i\varphi(n_M,n_L-1)}(t_A^*t_B^*)\alpha(n_M,n_L-1) = \\ = e^{i(\varphi_M+\varphi_U)}(-r_A^*r_B)\alpha(n_M-1,n_L) + e^{i(\varphi_L+\varphi_U)}(t_A^*t_B^*)\alpha(n_M,n_L-1).\end{aligned} \quad (2.26)$$

Reusing the symbols n and k from Eq. (2.6), we can define

$$a_{n,k} = \alpha(n_M,n_L) \quad (n \equiv k \pmod 2) \quad (2.27)$$

and refine the relation to

$$\begin{aligned}a_{n,k} = e^{i(\varphi_M+\varphi_U)}(-r_A^*r_B)a_{n-1,k+1} + e^{i(\varphi_L+\varphi_U)}(t_A^*t_B^*)a_{n-1,k-1} = C_1a_{n-1,k+1} + C_2a_{n-1,k-1}, \\ C_1 = e^{i(\varphi_M+\varphi_U)}(-r_A^*r_B) \\ C_2 = e^{i(\varphi_L+\varphi_U)}(t_A^*t_B^*),\end{aligned} \quad (2.28)$$

with direct formal analogy to Eq. (2.25). The main two differences are that

- the constants C_1 and C_2 are complex,
- we found a recurrence relation for amplitudes, not probabilities.

Due to the particular behaviour at $n = 1$, it is necessary to specify the initial conditions no sooner than at $n = 2$. Their complete set is then

$$\begin{aligned} a_{2,-2} &= \alpha(2,0) = -e^{i\varphi(2,0)} r_A^* r_B t_A t_B \\ a_{2,0} &= \alpha(1,1) = e^{i\varphi(1,1)} (T_A T_B + R_A R_B - 1) \\ a_{2,2} &= \alpha(0,2) = -e^{i\varphi(0,2)} r_A r_B^* t_A^* t_B^*, \end{aligned} \tag{2.29}$$

and we must keep Eq. (2.24) as special cases.

However, a mathematically equivalent approach is to say that the system is simulating *three* random walks which interfere. These three walks start at both different positions and different times. To distinguish from the previous notation, we will use tildes to denote their respective initial conditions:

$$\begin{aligned} \tilde{a}_{1,-1} &= a_{1,-1} = \alpha(1,0) = e^{i\varphi_M} t_A t_B \\ \tilde{a}_{1,1} &= a_{1,1} = \alpha(0,1) = -e^{i\varphi_L} r_A r_B^* \\ \tilde{a}_{2,0} &= a_{2,0} - (C_1 a_{1,1} + C_2 a_{1,-1}) = -e^{i\varphi(1,1)}. \end{aligned} \tag{2.30}$$

Note that the presence of nonzero $\tilde{a}_{2,0}$ prevents Eqs. (2.29) to be extended back to $n = 1$.

These relations allow us to claim that the system under study undergoes a special coinless quantum random walk. This is new since in the theory of quantum walk on a line, a nontrivial quantum walk without a coin degree of freedom is excluded by the No-Go Lemma mentioned in Sec. 1.1. In our case, this lemma is circumvented by changing the fundamental approach to a physical representation of the random walk time and position. However, this kind of quantum walk has limited mathematical possibilities since all the interference is simply additive. Despite the fact that the constants C_1 and C_2, from Eq. (2.28), are complex, their phases have no observable effect on the outcome. We can tell so by taking the square of the absolute value of Eq. (2.23):

$$\begin{aligned} P(n_M, n_L) = (R_A R_B)^{n_M - 1} (T_A T_B)^{n_L - 1} \times \\ \times \left(\binom{n-1}{n_L} T_A T_B + \binom{n-1}{n_M} R_A R_B - \binom{n-2}{n_M - 1} \right)^2. \end{aligned} \tag{2.31}$$

Note that no phase shifts affect this probability, it is expressed completely in terms of the classical parameters of the two beam splitters. The reason for this is that every possible scenario taken by the photon goes through every phase shift a fixed number of times. As we considered no time dependence of these phase shifts, every term in the path sum gains exactly the same phase and thus they can only interfere trivially.

2.6 Probability normalization

As the random walk iterations are nothing more than imaginary divisions of the photon's output time, the sum of probabilities $P(n_M, n_L)$ over one iteration, given by the condition $n_M + n_L = n = \text{const.}$, is not 1. Instead, the normalization

$$\sum_{\substack{n_M, n_L \in \mathbb{N}_0 \\ n_M + n_L > 0}} P(n_M, n_L) = 1 \tag{2.32}$$

holds unless we assume some possible losses inside the interferometer, in which case there would be a $\leq$ sign.

We can still consider $P(n_M, n_L)$ in the range of one iteration to be *relative probabilities* but then it is necessary to normalize them by multiplying all of them by a common factor of $1/C(n)$ where

$$C(n) = \sum_{n_M+n_L=n} P(n_M, n_L). \tag{2.33}$$

In the following, we will evaluate this sum.

Let us rewrite the probability (2.31) in terms of new simplifying parameters T and R, where

$$\begin{aligned} T &= T_A R_A, \\ R &= R_A R_B : \end{aligned} \tag{2.34}$$

$$P(n_M, n_L) = R^{n_M-1} T^{n_L-1} \left(\binom{n-1}{n_L} T + \binom{n-1}{n_M} R - \binom{n-2}{n_M-1} \right)^2. \tag{2.35}$$

Furthermore, we can rewrite the constraint $n_M + n_L = n$ to express n_L using n_M:

$$P(n_M, n-n_M) = R^{n_M-1} T^{n-n_M-1} \left(\binom{n-1}{n_M-1} T + \binom{n-1}{n_M} R - \binom{n-2}{n_M-1} \right)^2. \tag{2.36}$$

In order to find the normalization constant (2.33), we need to evaluate the sum

$$C(n) = \sum_{k=0}^{n} R^{k-1} T^{n-k-1} \left(\binom{n-1}{k-1} T + \binom{n-1}{k} R - \binom{n-2}{k-1} \right)^2. \tag{2.37}$$

The expression can be expanded to several sums of the form

$$R^a T^b \sum_{k=0}^{n} \binom{n_1}{k-k_1} \binom{n_2}{k-k_2} R^k T^{n-k}, \quad k_{1,2} \in \{0, 1\}, \tag{2.38}$$

which strongly resembles the left hand side of the binomial theorem but differs in containing a product of two binomial coefficients instead of one. This difference means that we need special functions to simplify the sum. The most straightforward way is to rewrite the expression to a hypergeometric function [21,22], which gives

$$\begin{aligned} \sum_{k=0}^{n} \binom{n_1}{k} \binom{n_2}{k} R^k T^{n-k} &= T^n \, {}_2F_1\left(-n_1, -n_2; 1; \frac{R}{T}\right) \\ \sum_{k=0}^{n} \binom{n_1}{k} \binom{n_2}{k-1} R^k T^{n-k} &= n_1 R T^{n-1} \, {}_2F_1\left(1-n_1, -n_2; 2; \frac{R}{T}\right), \end{aligned} \tag{2.39}$$

if $T \neq 0$. Note that if $T = 0$, we can take a limit of the right hand side as T approaches 0. This is justified by noticing that Eq. (2.37) is a polynomial in T and R and thus a continuous function.

These expressions can be alternatively rewritten using Jacobi polynomials or, in some special cases, Legendre polynomials [23,24], nevertheless, neither of these expressions can be considered a closed form.

The complete expression for $C(n)$ can be found this way to be

$$\begin{aligned} C(n) = {} & T^{n-1}(T+R)\,{}_2F_1(1-n,1-n;1;x) + \\ & + T^{n-2}\Big({}_2F_1(2-n,2-n;1;x) + 2(n-1)RT\,{}_2F_1(1-n,2-n;2;x) + \\ & - 2T\,{}_2F_1(1-n,2-n;1;x) - 2(n-1)R\,{}_2F_1(2-n,2-n;2;x)\Big), \end{aligned} \tag{2.40}$$

where $x = R/T$.

This expression can generally be simplified only in two special cases, $x = 0$ and $x = 1$. Because of the symmetry of swapping T and R in Eq. (2.37), it also has a limit as x approaches $+\infty$ which is equal to the value at $x = 0$.

The $x = 0$ case corresponds to a degenerate case $R = 0$ or, by the indicated symmetry, $T = 0$, where one or both of the beam splitters are completely transient or completely reflective. If both beam splitters are degenerate in this way, there is only one possible way the photon can take and thus only one possible escape time and its probability is one. No features of a random walk can be observed in this case at all.

Similarly, there is no interference even if only one of the two beam splitters is nondegenerate. In that case, the system can be fully described using the idea of a pulse which is attenuated by the same factor after every loop. In each case, there will be only one kind of time difference between the possible escape times (making the pattern a simple lattice without the fine division) and the escape probability will follow a simple exponential decay rule. Since there are no features of a quantum walk again, there is no need to go much into details.

Let us focus on the $x = 1$ case, or $T = R$. We note that this condition means that the transmittance of one beam splitter equals the reflectivity of the other one and *vice versa*. We will see another interesting property of such a configuration later.

In this case, the sum in Eq. (2.38) can be computed in closed form using the Chu-Vandermonde's identity [23]. It can also be found, along with a proof, as Theorem 6 in App. B. The result is

$$\sum_{k=0}^{n} \binom{n_1}{k-k_1}\binom{n_2}{k-k_2} = \binom{n_1+n_2}{n_2+k_2-k_1} \tag{2.41}$$

and consequently

$$\begin{aligned} C(n) &= T^{n-2}\left(2T^2\binom{2n-2}{n-1} + 2T^2\binom{2n-2}{n} + \binom{2n-4}{n-2} - 2T\left(\binom{2n-3}{n-1} + \binom{2n-3}{n-2}\right)\right) = \\ &= T^{n-2}\left(2T^2\binom{2n-1}{n} - 2T\binom{2n-2}{n-1} + \binom{2n-4}{n-2}\right) = \\ &= T^{n-2}\binom{2n-4}{n-2}\left(2T^2\frac{(2n-4)(2n-3)(2n-2)}{(n-2)^2(n-1)} - 2T\frac{(2n-3)(2n-2)}{(n-2)^2} + 1\right) = \\ &= T^{n-2}\binom{2n-4}{n-2}\left(16T^2 - 8T + 1 + O(n^{-1})\right). \end{aligned} \tag{2.42}$$

In order to find some asymptotic estimate, we can use Stirling's approximation formula [25,26] to find that

$$\binom{2n-4}{n-2} = \frac{2^{2n-4}}{\sqrt{(n-2)\pi}} \left(1 + O(n^{-1})\right). \tag{2.43}$$

The formula for $C(n)$ then becomes

$$\begin{aligned} C(n) &= T^{n-2} \frac{4^{n-2}}{\sqrt{(n-2)\pi}} \left(16T^2 - 8T + 1 + O(n^{-1})\right) \left(1 + O(n^{-1})\right) = \\ &= \frac{(4T)^{n-2} \left((4T-1)^2 + O(n^{-1})\right)}{\sqrt{(n-2)\pi}} \left(1 + O(n^{-1})\right) \end{aligned} \tag{2.44}$$

for $0 < T < \frac{1}{4}$. Therefore, the decay of the escape probability, taken as a function of the iteration count n, is approximately exponential with a quotient of $4T$.

After the normalization, we can define the probability $P_{n,k}$ of finding the walker after n steps on the position k as

$$P_{n,k} = C(n)^{-1} P(n_M, n_L) \quad (n \equiv k \pmod 2), \tag{2.45}$$

where n_M and n_L are linked to n and k via Eq. (2.6). The general shape of the probability distribution over all possible positions k for given n is illustrated in Fig. 6.

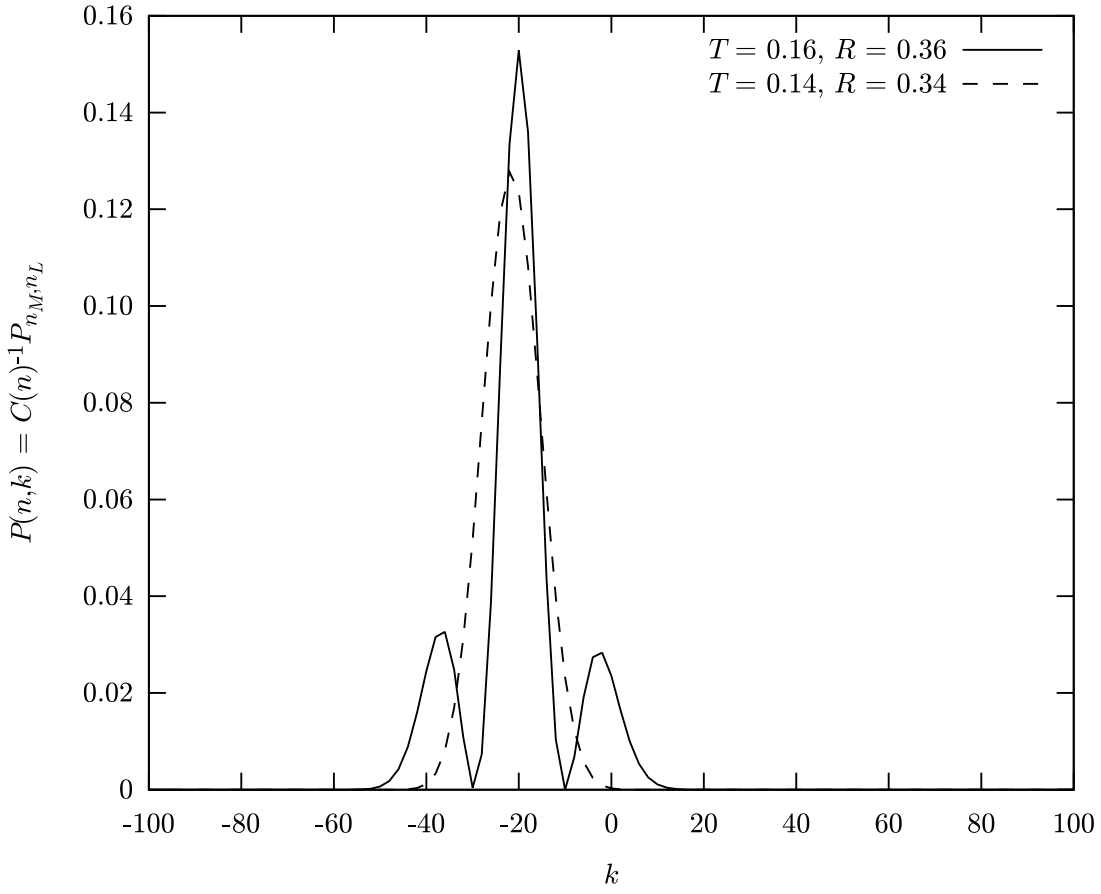

Fig. 6: The two most common shapes of the probability distribution of the random walk, Eq. (2.45). Both plots were computed after $n = 100$ steps. Note that there can be up to three peaks located near a common center, however, after a small change in the T and R parameters, the side peaks can vanish. Only even parity positions are plotted, the probability is zero on odd parity ones.

2.7 Parameter optimization

In order to observe the signs of a random walk in the escape time probability distribution, it is desirable to reach as high values of n as possible since a higher number of iterations allows us to resolve finer details of the distribution shape.

For the same reason, it is important to reduce the probability of the photon escaping in the first two iterations where the behaviour is rather trivial. Therefore, let us compute the total probability of escaping at $n = 1$ or $n = 2$ directly,

$$\begin{aligned} P_{1+2} &= P_{1,0} + P_{0,1} + P_{2,0} + P_{1,1} + P_{0,2} = \\ &= T + R + TR + (T + R - 1)^2 + TR = \\ &= T^2 + R^2 + 4TR - T - R + 1. \end{aligned} \tag{2.46}$$

We will attempt to minimize this probability by altering the beam splitter parameters.

First, however, let us emphasize here that the values of T and R can not be chosen independently. Starting from Eqs. (2.34) and (2.12), we can use the constrained optimization problem methods to find that

$$0 \leq R \leq (1 - \sqrt{T})^2 \tag{2.47 a}$$

or, equivalently,

$$0 \leq \sqrt{T} + \sqrt{R} \leq 1. \tag{2.47 b}$$

Thus the region reachable by all choices of beam splitter parameters T_A, T_B, R_A and R_B is limited by the lines $T = 0$, $R = 0$ and the curve $\sqrt{T} + \sqrt{R} = 1$.

Analyzing the function

$$f(T, R) = T^2 + R^2 + 4TR - T - R + 1 \tag{2.48}$$

due to these constraints reveals the following significant points:

- a saddle point at $T = R = \frac{1}{6}$ with function value of $\frac{5}{6}$,
- global maxima $f(0,0) = f(1,0) = f(0,1) = 1$,
- global minima $f\left(0, \frac{1}{2}\right) = f\left(\frac{1}{2}, 0\right) = \frac{3}{4}$ and a local minimum on the domain bound $f\left(\frac{1}{4}, \frac{1}{4}\right) = \frac{7}{8}$.

We can see most of these points fall into some of the degenerate cases listed in the previous section as one or both of the T and R parameters are zero or one. After leaving them out, we are left with only two of the extremal points, both lying on the line of $T = R$. We have found that the point $T = R = \frac{1}{6}$ is the local minimum of Eq. (2.48) on this domain subset, whereas the border points $T = R = \frac{1}{4}$ and $T = R = 0$ are local maxima.

Let us find the exact set of parameters yielding $T = R = \frac{1}{6}$. This gives the following system of equations:

$$\begin{aligned} T = T_A T_B &= \frac{1}{6}, \\ R = R_A R_B &= \frac{1}{6}, \\ T_A + R_A &= 1, \\ T_B + R_B &= 1. \end{aligned} \tag{2.49}$$

There are two possible solutions,

$$\begin{aligned} T_A = R_B &= \frac{1 \pm \sqrt{\frac{1}{3}}}{2}, \\ R_A = T_B &= \frac{1 \mp \sqrt{\frac{1}{3}}}{2}. \end{aligned} \tag{2.50}$$

As we have computed above, in this configuration, there is a probability of one in six for every photon to survive to iterations $n \geq 3$. As this is a saddle point, there are configurations allowing higher probability outside the $T = R$ line, however, no other local extrema occurs in this region prior to reaching one of the trivial cases.

Another task would be to optimize the parameters for the best asymptotic behaviour. From the previous section, we know the result when we restrict ourselves to the case $T = R$: the optimal point under this condition is $T = R = \frac{1}{4}$, the other significant point found above. On average, seven of eight input photons escape in the first two iterations in such configuration, which is worse than the previous special case approximately by 4% but the tail of the distribution is more well-behaved.

Moreover, we can note that this point forms an intersection of the line $T = R$ and the border curve $\sqrt{T} + \sqrt{R} = 1$. We already know from above that the former means $T_A = R_B$ and $R_A = T_B$, similarly, the latter is equivalent to $T_A = T_B$ and $R_A = R_B$. Therefore, we do not need to solve another system of equations: this special case is reached when both the beam splitters are balanced,

$$T_A = R_A = T_B = R_B = \frac{1}{2}. \tag{2.51}$$

Eq. (2.44) gives us a very good description of the $C(n)$ function in this special case. However, if we were interested only in the decay rate (ignoring the overall prefactor), this coefficient can be found generally. As a corollary of Theorem 7 in App. B, we can find that $C(n)$ behaves in higher n approximately as a geometric progression with a quotient of

$$T\left(\sqrt{\frac{R}{T}} + 1\right)^2 = \left(\sqrt{R} + \sqrt{T}\right)^2.$$

In order to minimize the exponential decay, one would want to maximize this expression. From Eq. (2.47 b), we can note that the maximum of this expression is 1 and it is reached exactly on the domain border curve $\sqrt{T} + \sqrt{R} = 1$. However, we emphasize that a unit exponential quotient does not mean that the $C(n)$ function approaches a constant limit—only that the decay is slower than exponential.

2.8 Mean position of the walker

In this section, we will study the behaviour of the mean position of the walker, which is one of the main characteristics of any random walk. The computation will also reveal some estimates on the spread in the position.

Up to a normalization constant, the probability of finding the walker on position k after n steps of the modelled random walk is given by Eq. (2.35), where the n_M and n_L indices are linked with n and k via Eq. (2.6). The mean position of the walker is then given by

$$\langle k \rangle = \frac{\sum\limits_{n_M=0}^{n} \sum\limits_{n_L=n-n_M} (n_L - n_M) P(n_M, n_L)}{\sum\limits_{n_M=0}^{n} \sum\limits_{n_L=n-n_M} P(n_M, n_L)}. \tag{2.52}$$

We are interested in the limit linear speed of the walker, that is,

$$s = \lim_{n \to +\infty} \frac{\langle k \rangle}{n}. \tag{2.53}$$

In order to solve this problem, we will need to make some observations about the probability distribution.

After expanding Eq. (2.35), we will obtain several terms of the form

$$R^a T^b \binom{n - \nu_1}{n_M - \mu_1} \binom{n - \nu_2}{n_M - \mu_2} R^{n_M} T^{-n_M}. \tag{2.54}$$

After introducing $x = R/T$, we can use Lemma 8 from App. B to find that this term has a maximum near

$$n_{M_0} = \left[\frac{\sqrt{x}}{\sqrt{x} + 1} n \right], \tag{2.55}$$

where $[x]$ denotes the nearest integer to x. Since this expression is independent of the small shifts in the binomial coefficients, μ_i and ν_i, the same result holds for every term in the expanded Eq. (2.35) and thus we can assume that the total probability also reaches its maximum in the neighbourhood of n_{M_0}. Note that this is not automatically true as some of the terms have negative sign and could hypothetically cancel out the positive ones.

In order to refine this statement, we can conjecture the following lemma: Let $\alpha \in (\frac{1}{2}, 1)$, denote $\Delta n_M = \lfloor n^\alpha \rfloor$. Then an asymptotically negligible part of the probability is distributed outside the interval $\langle n_{M_0} - \Delta n_M, n_{M_0} + \Delta n_M \rangle$, that is,

$$\lim_{n \to +\infty} \frac{\sum\limits_{n_M=n_{M_0}-\Delta n_M}^{n_{M_0}+\Delta n_M} P(n_M, n - n_M)}{\sum\limits_{n_M=0}^{n} P(n_M, n - n_M)} = 1. \tag{2.56}$$

The complete proof is not presented as it is long and technical. Its main idea is to take a complement of the ratio to 1, estimate all the factorials in the binomial coefficients in Eq. (2.35) using the Stirling approximation and study the limit of logarithm of this sequence. The rest is a straightforward procedure of usual techniques for computing limits of number sequences.

Using this lemma, we can return to Eqs. (2.52) and (2.53). We can combine the two equations into

$$s = \lim_{n\to+\infty} \frac{\sum_{n_M=0} \left(1 - \frac{2n_M}{n}\right) P(n_M, n-n_M)}{\sum_{n_M=0}^{n} P(n_M, n-n_M)}. \tag{2.57}$$

We note that as the factor of $1-\frac{2n_M}{n}$ is bounded, the above theorem can be used directly to restrict both the sums to the interval $\langle n_{M_0} - \Delta n_M, n_{M_0} + \Delta n_M \rangle$. We then estimate this factor by

$$1 - \frac{2(n_{M_0} + \Delta n_M)}{n} \leq 1 - \frac{2n_M}{n} \leq 1 - \frac{2(n_{M_0} - \Delta n_M)}{n} \tag{2.58}.$$

As neither of the bounds depends on n_M, they can be factored out of the sum in the numerator, leaving the same sum in the numerator as in the denominator. After cancelling them with each other, we obtain estimates for s:

$$1 - \frac{2(n_{M_0} + \Delta n_M)}{n} \leq s \leq 1 - \frac{2(n_{M_0} - \Delta n_M)}{n} \tag{2.59}.$$

To find the asymptotic speed, we need to take limit as n approaches $+\infty$ on both sides. Recall that n_{M_0} and Δn_M are functions of n. It follows from the corresponding definitions that

$$\lim_{n\to+\infty} \frac{n_{M_0}}{n} = \frac{\sqrt{x}}{\sqrt{x}+1} \tag{2.60 a}$$

and that

$$\lim_{n\to+\infty} \frac{\Delta n_M}{n} = 0. \tag{2.60 b}$$

Therefore, both the bounds have the same limit value, giving

$$s = 1 - 2\frac{\sqrt{x}}{\sqrt{x}+1} = \frac{1-\sqrt{x}}{1+\sqrt{x}}. \tag{2.61}$$

Let us compute s in the two significant cases introduced in Sec. 2.7. First, if $T = R$, i.e., $T_A = R_B$ and $T_B = R_A$, then $x = R/T = 1$ and $s = 0$, i.e., for this particular connection between the beam splitter parameters, the mean position of the walker stays in the middle of the line.

The second important case was $T_A = T_B$ and $R_A = R_B$. In this case, the square root of x can be easily simplified:

$$\sqrt{x} = \sqrt{\frac{R}{T}} = \sqrt{\frac{R_A^2}{T_A^2}} = \frac{R_A}{T_A} \tag{2.62}.$$

The asymptotic speed can then be simplified as

$$s = \frac{T_A - R_A}{T_A + R_A} = T_A - R_A. \tag{2.63}$$

Note that this provides an easy way of finding the interferometer parameters to obtain a quantum walk for an arbitrary given $s \in \langle -1, 1 \rangle$.

The above theorem also indicates that the variance of the position distribution is $O(n^{1+\varepsilon})$ for any $\varepsilon > 0$. The proof is analogous but we obtain an upper bound only. This property reminds of a classical random walk, which has a variance of const. $\times\, n$.

2.9 Relation to coherent states

In this section, we will point out a correspondence between the one photon and coherent state operation of the interferometer, justifying the model used in Sec. 2.3. For this purpose, we will need to replace the detector by an infinite output line continuing in one direction, as explained in Sec. 2.3. To be accurate, we note that the derivation below is valid only in an idealized case where no decoherence is taken into account.

After a given time, the initial state $|\psi_i\rangle$ of the photon is transformed to a linear combination of some number of wave packets inside the loop and some number of wave packets propagating on the output line. Under the conditions given above, all these wave packets are finitely supported and spatially separated. We will also assume that the time is chosen such that the wave function vanishes in the vicinity of the beam splitters.

Therefore, the state can be written as

$$U(t)|\psi_i\rangle = \sum_{k=1}^{N} \alpha_k |\psi_o\rangle_{t_k} + \varepsilon |r\rangle, \tag{2.64}$$

where $|\psi_o\rangle_{t_k}$ denotes a wave packet state on the output line which passed the location of the detector at the escape time of t_k. The state $|r\rangle$ describes the renormalized part of the wave function supported on the M, L and U arms. Due to the spatial separation, all the $|\psi_o\rangle_{t_k}$ and the remainder $|r\rangle$ are mutually orthogonal.

We can use the notation of App. A to rewrite Eq. (2.64) to operator form. That is, we will make a second quantization of the state space and define creation operators for all the states used in that equation:

$$\begin{aligned} |\psi_i\rangle &= a_i^\dagger |0\rangle \\ |\psi_o\rangle_{t_k} &= a_{t_k}^\dagger U(t)|0\rangle \\ |r\rangle &= a_r^\dagger U(t)|0\rangle, \end{aligned} \tag{2.65}$$

where $|0\rangle$ is the vacuum state. After factoring $|0\rangle$ out, Eq. (2.64) becomes

$$U(t) a_i^\dagger U(t)^\dagger = \sum_{k=1}^{N} \alpha_k a_{t_k}^\dagger + \varepsilon a_r^\dagger. \tag{2.66}$$

We are interested in replacing the initial one photon state $|\psi_i\rangle$ by a coherent pulse based on this state, that is,

$$|\alpha\rangle_i = \exp(\alpha a_i^\dagger - \alpha^* a_i)|0\rangle. \tag{2.67}$$

In order to find the transformation of this state under $U(t)$, we first need to find an adjoint of Eq. (2.66),

$$U(t)a_i U(t)^\dagger = \sum_{k=1}^{N} \alpha_k^* a_{t_k} + \varepsilon^* a_r, \tag{2.68}$$

and use it to express the transformation of the linear combination

$$U(t)(\alpha a_i^\dagger - \alpha^* a_i)U(t)^\dagger = \sum_{k=1}^{N} (\alpha\alpha_k a_{t_k}^\dagger - \alpha^*\alpha_k^* a_{t_k}) + (\alpha\varepsilon a_r^\dagger - \alpha^*\varepsilon^* a_r). \tag{2.69}$$

As the $|\psi_o\rangle_{t_k}$ states are orthogonal and $|r\rangle$ is orthogonal to all of them, the linear combinations of their creation and annihilation operators mutually commute. This enables us to compute

$$U(t)\exp(\alpha a_i^\dagger - \alpha^* a_i)U(t)^\dagger = \prod_{k=1}^{N} \exp(\alpha\alpha_k a_{t_k}^\dagger - \alpha^*\alpha_k^* a_{t_k}) \exp(\alpha\varepsilon a_r^\dagger - \alpha^*\varepsilon^* a_r). \tag{2.70}$$

When the right hand side is applied on the vacuum vector, it creates a product of coherent states in the modes defined by the vectors $|\psi_o\rangle_{t_k}$ and some coherent excitations inside the delay loop. Thus, every term $\alpha_k|\psi_o\rangle_{t_k}$ in the linear combination (2.66) became a coherent pulse at the same location and having an amplitude of $\alpha\alpha_k$ in this operation. The intensity of this partial pulse has an $|\alpha_k|^2$ ratio to the intensity of the input pulse. In other words, the probability of detecting one photon at a given time t_k, as described in Sec. 2.3, becomes exactly the intensity of a partial pulse measured at the same time if we use a coherent state at the input. Hence, we can safely claim that there is an exact correspondence between the two experimentally different approaches.

2.10 Summary

Let us summarize the results obtained in this chapter. The study of the system depicted in Fig. 1 showed that under certain conditions, quantum walk behaviour can be observed in the output. All the iteration-position pairs are merged to a single time line, and thus all the probability amplitudes of the walk can be observed without changing the experiment layout and/or external conditions. The walk can be described using a recurrence relation between the probability amplitudes.

In order to reconstruct the quantum walk, the output must be split into a sequence of time bins and probability distribution of finding the walker on the possible positions must be renormalized within each of these bins. The resulting walk scenario displays similar position and variance dependence on the number of steps as a classical random walk on a line, although that the probability distribution is not Gaussian. The asymptotic speed of the walker was computed exactly.

Several optimization problems were discussed with the result that there is a straightforward way of reaching higher iterations of the walk with enough fidelity. Under this optimality condition, one degree of freedom is still left, allowing to reach any bias of the walk.

Chapter 3
Quantum walk using polarization as a coin

In this chapter, we will focus on the possibilities of realizing a coined discrete time quantum walk in a similar way as in Chap. 2.

We note that parts of this chapter, namely sections 3.5, 3.6 and 3.7, are based on the results of Andreas Schreiber, Katiuscia Cassemiro and Christine Silberhorn from the Max Planck Institute for the Science of Light, Erlangen, Germany. We claim no connection to the design and/or implementation of the particular experiment.

3.1 The polarization degree of freedom

It follows from the fundamentals of quantum optics that a scalar wave function does not represent the state of one photon fully. There is one additional degree of freedom corresponding to *polarization* of the electromagnetic field [27], as known from classical wave optics. The existence of this degree of freedom results in extension of the former Hilbert space by taking a tensor product with a two-dimensional space, $\mathbb{C}^2$. The resulting system is isomorphic to a compound system consisting of a spinless particle and one qubit.

As an example of using only one part of this compound system, let us show why polarization could be ignored in Chap. 2. This is a nontrivial question since in a compound system, generally, one can not consistently define states of the individual subsystems without allowing a system to be in a *mixed state*. For this purpose, we must convert the above description using elements of the Hilbert space to a more general approach using the *density matrix*, or a *statistical operator*, to describe the state of a quantum system [28].

In this formalism, we define for any ket $|\psi\rangle \in \mathcal{H}$ a corresponding *pure state* as the orthogonal projector on the one-dimensional linear hull of $|\psi\rangle$:

$$E_{|\psi\rangle} = |\psi\rangle\langle\psi|. \tag{3.1}$$

Note that this assignment is not injective: kets differing in their global phase give the same pure state. This is no contradiction, however, since such states are physically equivalent. By allowing mixed states, the state space expands to a convex hull of all pure states. Mixed states do not correspond to any wave function, but they can be viewed as probability distributions over more than one pure states the system can be in.

If the state of a compound system, ϱ, can be factorized as $\varrho_1 \otimes \varrho_2$, we can equivalently claim that the first and second subsystem are in states ϱ_1 and ϱ_2, respectively. However, this is not always the case: by taking convex combinations of factorized states, we generally obtain states which can not be factorized. To assign some states to the subsystems, one uses a *partial trace* operator [28]. For the above system composed of two subsystems, we say that the first and second subsystems are

in states $\mathrm{Tr}_1\,\varrho$ and $\mathrm{Tr}_2\,\varrho$, respectively. Note that generally, part of the information contained in ϱ is lost when only its partial traces are known. If and only if one of the of the partial traces of ϱ is a pure state, we can reconstruct ϱ as

$$\varrho = (\mathrm{Tr}_1\,\varrho) \otimes (\mathrm{Tr}_2\,\varrho). \tag{3.2}$$

Returning to the case of Chap. 2, we note that there are no polarization-active elements in the experimental setup (see Fig. 1). Thus, the propagator of the system, U, factorizes to a tensor product $U_1 \otimes U_2$, where U_1 acts on the position state space and U_2 on the polarization state space of the photon. Let the initial state be factorized as

$$\varrho_i = \varrho_1 \otimes \varrho_2. \tag{3.3}$$

In the density matrix description, the propagator U transforms this state into

$$\varrho_o = U\,\varrho_i U^\dagger. \tag{3.4}$$

By substituting the above factorizations for all the involved operators, we obtain ϱ_o in a factorized form

$$\varrho_o = (U_1 \otimes U_2)(\varrho_1 \otimes \varrho_2)(U_1^\dagger \otimes U_2^\dagger) = (U_1 \varrho_1 U_1^\dagger) \otimes (U_2 \varrho_2 U_2^\dagger). \tag{3.5}$$

From this equation, we can see that both the subsystems evolve independently of each other, according to the partial propagators U_1 and U_2. Especially, if ϱ_1 was a pure state corresponding to a ket $|\psi_i\rangle$, then

$$\mathrm{Tr}_1\,\varrho_o = U_1 \varrho_1 U_1^\dagger \tag{3.6}$$

is a pure state again, corresponding to $U_1|\psi_i\rangle$, regardless of whether the polarization was pure or mixed.

3.2 An interferometer implementing a coined quantum walk

In the following, we would like to introduce an experimentally realizable linear optics implementation of the coined quantum walk on a line, as described in Sec. 1.1, using a similar basic idea as in Chap. 2. According to Sec. 3.1, the polarization space is suited perfectly to be used as the coin space in such experiment.

In contrast to Fig. 1, the "walker" should take the shorter or longer path according to his polarization. Thus, we will replace the beam splitters A and B by *polarizing beam splitters* which split the two orthogonal polarization states of an incoming beam in two directions. However, one additional normal beam splitter must be added to in-couple a pulse into the interferometer and out-couple it into a detector. We will assume that it is nontrivial, i.e., both its transmittance and reflectivity are nonzero. A schematic of the resulting layout is shown in Fig. 7.

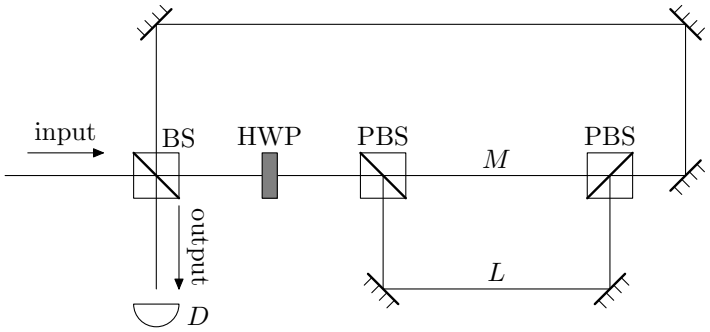

Fig. 7: The second configuration. BS denotes a classic beam splitter, PBS a polarizing beam splitter, HWP a half-wave plate and D a detector.

A coherent pulse or one photon is inserted into the input arm in a precise polarization state and couples into the loop with relative intensity, or probability, given by the transmittance of the beam splitter BS. It first reaches the half-wave plate HWP, which mixes the polarization states and thus represents the action of the C gate. As shown in Sec. 3.3, HWP can represent a whole class of gates with spectrum $\{1, -1\}$. It can be replaced by another wave plate if another relative phase shift is required. By allowing more than one wave plate, any one-qubit gate is obtainable, as follows from decomposition of unitary matrix into a product of rotational matrices [28]. The pulse then splits on the left hand PBS in the preferred polarization basis, and the lower arm L in Fig. 7 obtains a relative time delay to the middle arm M. The polarization must be maintained reliably so that at the right hand PBS, a photon coming from either arm continues in the main loop. After completing the loop, there is some probability of escaping to the detector, otherwise the cycle is repeated for another iteration of the quantum walk.

3.3 The mathematical model

In order to describe the experiment in Fig. 7 mathematically, we will reuse most of the results of Sec. 2.3. However, we must adjust them to include the polarization degree of freedom. Let $\mathcal{H}_S$ denote the "position" Hilbert space, defined analogously as in Sec. 2.3, let $\mathcal{H}_C = \mathbb{C}^2$ be the polarization Hilbert space. The complete Hilbert space of the system can be written as $\mathcal{H} = \mathcal{H}_S \otimes \mathcal{H}_C$.

To specify a matrix element of an operator fully, we would have to specify position and polarization kets for both the initial and final state. Alternatively, if we use the previous notation,

$$\langle \psi_1 | U | \psi_2 \rangle, \quad |\psi_1\rangle, |\psi_2\rangle \in \mathcal{H}_S, \tag{3.7}$$

this object behaves as an operator on $\mathcal{H}_C$ and could be specified by a matrix in an appropriate basis. We will call it a *partial matrix element*.

Let the preferred basis of $\mathcal{H}_C$ be specified by the polarizing beam splitters. As noted above, these elements transmit one polarization state and reflect the orthogonal one. The basis which determines this behaviour is defined by the *plane of incidence*, spanned by two vectors: a normal to the plane of the polarizing beam splitter and the propagation vector of the incident beam. The reflected

polarization state is called the s-polarization while the transmitted the p-polarization. This comes from the German words for perpendicular and parallel, respectively, speaking about the relative orientation of the electric intensity vector due to this plane. We will define an orthonormal basis denoted as $\{|p\rangle, |s\rangle\}$ accordingly.

New elements in the configuration are the half-wave plate and the polarizing beam splitters. The action of the half-wave plate HWP on an incoming pulse may be specified using an unitary matrix of rank 2 in the sense outlined above. However, the exact form of this matrix depends on the orientation of the plate, determined by the *optic axis*. If this axis is aligned with one of the preferred polarization directions, say p, the half-wave plate creates a relative $\pi/2$ phase shift between the polarizations, which can be written as the Pauli Z matrix in the preferred basis,

$$\sigma_Z = \begin{pmatrix} 1 & 0 \\ 0 & -1 \end{pmatrix}, \tag{3.8}$$

acting in $\mathcal{H}_C$. If the optical axis is rotated by an angle φ due to the p axis (the sense of measuring φ depends on what we consider the positive direction of the p and s axes), this matrix must be transformed to represent this basis change, resulting in

$$U_{\mathrm{HWP}} = \begin{pmatrix} \cos\varphi & -\sin\varphi \\ \sin\varphi & \cos\varphi \end{pmatrix} \begin{pmatrix} 1 & 0 \\ 0 & -1 \end{pmatrix} \begin{pmatrix} \cos\varphi & \sin\varphi \\ -\sin\varphi & \cos\varphi \end{pmatrix} = \begin{pmatrix} \cos 2\varphi & \sin 2\varphi \\ \sin 2\varphi & -\cos 2\varphi \end{pmatrix}. \tag{3.9}$$

For example, if $\varphi = \pi/8$, then we obtain the Hadamard matrix,

$$H = \frac{1}{\sqrt{2}} \begin{pmatrix} 1 & 1 \\ 1 & -1 \end{pmatrix}. \tag{3.10}$$

We will describe the whole polarizing beam splitter delay loop as one element in this model. Let t_M and t_L denote again the time needed to travel the arms M and L, respectively. Let $|\psi_1\rangle$ and $|\psi_2\rangle$ denote wave packets right before and after the delay loop, analogously to Fig. 4. For the initial states with their $\mathcal{H}_S$ component $|\psi_1\rangle$, time evolution gives

$$\begin{aligned} U(t_M)|\psi_1\rangle|p\rangle &= e^{\varphi_p}|\psi_2\rangle|p\rangle, \\ U(t_L)|\psi_1\rangle|s\rangle &= e^{\varphi_s}|\psi_2\rangle|s\rangle, \end{aligned} \tag{3.11}$$

which can be rewritten using the notation of partial matrix elements as

$$\begin{aligned} \langle\psi_2|U(t_M)|\psi_1\rangle &= e^{\varphi_p} E_{|p\rangle}, \\ \langle\psi_2|U(t_L)|\psi_1\rangle &= e^{\varphi_s} E_{|s\rangle}, \end{aligned} \tag{3.12}$$

if the time difference $|t_L - t_M|$ is large compared to the duration of the pulse, t_p.

For further considerations, we will give names to several other vectors in the position space. Their geometrical meaning is displayed in Fig. 8.

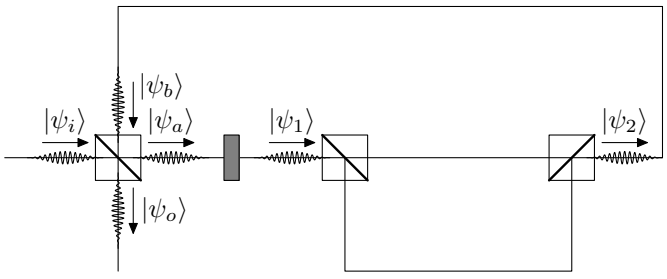

Fig. 8: The selected states in $\mathcal{H}_S$ needed for the mathematical description of the experiment in Fig. 7.

3.4 The path sum and the recurrence relation

Similarly as in Sec. 2.4, we will aim to describe the operation of this experimental configuration using the one photon dynamics and the path sum approach. The derivation will be simplified due to the fact that any complete loop must start (in terms of an optical path) at the location of $|\psi_a\rangle$ and end in the location of $|\psi_b\rangle$ according to Fig. 8. Any complete optical path in the studied layout is composed of a sequence of these loops, with only an in-coupling and out-coupling added on its beginning and its end, respectively, and can be described using a word composed of letters M and L to denote the order of the loops.

We will define t'_M and t'_L as the times needed to take one complete loop via the M or the L arm, respectively. The time needed to travel a path described by any word containing M and L letters in the count of n_M and n_L is then given by

$$t = n_M t'_M + n_L t'_L, \tag{3.13}$$

up to a small constant term corresponding to the in- and out-coupling. Also, we will assume the algebraic independence of t'_M and t'_L in the sense pointed out in Sec. 2.2 in order to make this mapping injective, and use the symbols n and k from Eq. (2.6).

We can compose the path sum of the partial matrix elements of the propagator, introduced in Sec. 3.3. The irreducible matrix elements from Sec. 2.4 become two-dimensional linear transforms. Their multiplications must be viewed as operator compositions, or multiplications of matrices, and we must preserve the order of the factors.

Due to the experiment layout, there are only two main irreducible matrix elements,

$$\begin{aligned} \langle\psi_b|U(t'_M)|\psi_a\rangle &= e^{i\varphi_1}\langle\psi_2|U(t_M)|\psi_1\rangle e^{i\varphi_2}U_{\mathrm{HWP}} = e^{i\varphi_M}E_{|p\rangle}U_{\mathrm{HWP}}, \\ \langle\psi_b|U(t'_L)|\psi_a\rangle &= e^{i\varphi_1}\langle\psi_2|\,U(t_L)\,|\psi_1\rangle e^{i\varphi_2}U_{\mathrm{HWP}} = e^{i\varphi_L}E_{|s\rangle}U_{\mathrm{HWP}}, \end{aligned} \tag{3.14}$$

supported by the in-coupling, out-coupling and reflecting matrix elements of the beam splitter BS, which are insensitive of polarization and thus multiplies of the identity operator:

$$\begin{aligned} \langle\psi_a|U_{\mathrm{BS}}|\psi_i\rangle &= t, \\ \langle\psi_o|U_{\mathrm{BS}}|\psi_i\rangle &= r, \\ \langle\psi_a|U_{\mathrm{BS}}|\psi_b\rangle &= -r^*, \\ \langle\psi_o|U_{\mathrm{BS}}|\psi_b\rangle &= t^*. \end{aligned} \tag{3.15}$$

A photon inserted in the state $|\psi_i\rangle \otimes |z\rangle$ can be reflected directly to the detector with probability amplitude $\langle\psi_o|U_{\mathrm{BS}}|\psi_i\rangle = r$. This must be considered a special case. For all other escape times, we can compute the partial matrix element $\langle\psi_o|U(t)|\psi_i\rangle$ in a uniform manner. However, it can not be considered as a probability amplitude anymore since it is a linear operator, transforming the initial polarization state into a polarization state that could be measured on the escaped photon, and the

escape probability amplitude serves as a multiplicative factor. This element can be evaluated as follows:

$$\begin{aligned}\langle\psi_o|U(n_M t'_M + n_L t'_L)|\psi_i\rangle = \alpha(n_M, n_L) = \sum_W \alpha_W = \\ = \sum_W \langle\psi_o|U_{\mathrm{BS}}|\psi_b\rangle \left(\prod_{i=1}^{n-1} \left\langle\psi_b\right|U\left(t'_{W_{n+1-i}}\right)\left|\psi_a\right\rangle\langle\psi_a|U_{\mathrm{BS}}|\psi_b\rangle\right) \langle\psi_b|U(t'_{W_1})|\psi_a\rangle\langle\psi_a|U_{\mathrm{BS}}|\psi_i\rangle = \\ = tt^*(-r^*)^{n-1} \sum_W \prod_{i=1}^{n} \left\langle\psi_b\right|U\left(t'_{W_{n+1-i}}\right)\left|\psi_a\right\rangle,\end{aligned} \tag{3.16}$$

where a time-ordered product of the irreducible matrix elements from Eq. (3.14) is used. The sum denoted $\sum_W$ is taken over all words W composed of M and L letters in the counts n_M and n_L, respectively.

By factoring out the first term of the product and separating the cases of the two letters, we get for $n_M > 0$ and $n_L > 0$ the following recurrence relation for $\alpha(n_M, n_L)$:

$$\begin{aligned}\alpha(n_M, n_L) &= -r^*\langle\psi_b|U(t'_M)|\psi_a\rangle\alpha(n_M - 1, n_L) - r^*\langle\psi_b|U(t'_L)|\psi_a\rangle\alpha(n_M, n_L - 1) = \\ &= -r^* e^{i\varphi_M} E_{|p\rangle} U_{\mathrm{HWP}} \alpha(n_M - 1, n_L) - r^* e^{i\varphi_L} E_{|s\rangle} U_{\mathrm{HWP}} \alpha(n_M, n_L - 1).\end{aligned} \tag{3.17}$$

The validity of this relation can be extended to cases where either n_M or n_L are zero if we define

$$\alpha(n, -1) = \alpha(-1, n) = 0 \tag{3.18}$$

for all $n \in \mathbb{N}$. $\alpha(0, 0)$ is assumed to be defined consistently with Eq. (3.16) as $-tt^*(r^*)^{-1}$, despite the fact that it does not represent any actual matrix element.

To simplify Eq. (3.17), let us define a new operator

$$C = -\left(e^{i\varphi_M} E_{|p\rangle} + e^{i\varphi_L} E_{|s\rangle}\right) U_{\mathrm{HWP}}, \tag{3.19}$$

so that

$$E_{|p\rangle} C = -e^{i\varphi_M} E_{|p\rangle} U_{\mathrm{HWP}} \tag{3.20 a}$$

and

$$E_{|s\rangle} C = -e^{i\varphi_L} E_{|s\rangle} U_{\mathrm{HWP}}. \tag{3.20 b}$$

From the properties of orthogonal projectors, it also follows that C is unitary:

$$CC^\dagger = \left(e^{i\varphi_M} E_{|p\rangle} + e^{i\varphi_L} E_{|s\rangle}\right) U_{\mathrm{HWP}} U_{\mathrm{HWP}}^\dagger \left(e^{-i\varphi_M} E_{|p\rangle} + e^{-i\varphi_L} E_{|s\rangle}\right) = E_{|p\rangle} + E_{|s\rangle} = \mathbb{1}. \tag{3.21}$$

Using this operator, we can rewrite Eq. (3.17) in the form

$$\alpha(n_M, n_L) = r^* \left(E_{|p\rangle} C \alpha(n_M - 1, n_L) + E_{|s\rangle} C \alpha(n_M, n_L - 1)\right). \tag{3.22}$$

As a next step, we will introduce

$$a_{n,k} = (r^*)^{-n} \alpha(n_M, n_L)|z\rangle, \quad (n \equiv k \pmod 2), \tag{3.23}$$

which has the physical meaning of the non-normalized polarization state of the photon, if it is detected in the output arm at the escape time (3.13), where $|z\rangle$ denotes its initial polarization state—in other words, if the initial state of the photon is assumed to be $|\psi_i\rangle \otimes |z\rangle$. Also, the substitution (2.6) was made. Applying the operators on both sides of Eq. (3.22) on the ket $|z\rangle$, we obtain a recurrence relation for $a_{n,k}$:

$$a_{n,k} = E_{|p\rangle} C a_{n,k+1} + E_{|s\rangle} C a_{n,k-1}. \tag{3.24}$$

This formula has the same form as the propagator of a quantum walk on a line, as derived in [6]. We can compare Eq. (3.24) with a corresponding equation there:

$$\Psi(n, t+1) = M_+ \Psi(n-1, t) + M_- \Psi(n+1, t). \tag{3.25}$$

Here $\Psi(n,t)$ is the two-component vector of amplitudes of the walker being at point n at time t and M_+ and M_- is the coin matrix multiplied from the left by the orthogonal projector on the left and right chirality state, respectively. Also, $a_{n,k}$ is a mathematical object of the same kind as $\Psi(n,t)$, a vector in $\mathbb{C}^2$. In order to claim a physical correspondence of the studied system's evolution to this quantum walk, we should check the relation between the initial conditions of both recurrence relations.

In [6], the walker starts at both time and position zero. Thus, $\Psi(n,0)$ is nonzero only for $n = 0$, $\Psi(0,0)$ denotes the walker's initial chirality state. In our notation, the number of the random walk iteration is denoted by n and the position k. Analogously, $a_{0,k}$ can only be nonzero for $k = 0$ because other values of k would represent negative n_M or n_L when transformed back via Eq. (2.6). According to Eqs. (3.23) and (3.16),

$$a_{0,0} = \alpha(0,0)|z\rangle = -tt^*(r^*)^{-1}|z\rangle, \tag{3.26}$$

so this value is proportional to the initial state $|z\rangle$ with some complex factor.

Using these observations, we can conclude that the system models the quantum walk on a line as it was introduced in Sec. 1.1. The walk can be reconstructed a similar way to Sec. 2.6: collecting the output from all escape times into groups with the same n and renormalizing the probability in each of these bins.

In contrast to Sec. 2.6, probability normalization is much simpler. From the exact correspondence of the recurrence relations and the unitarity of the actual quantum walk, we know that the value of

$$S(n) = \sum_{k=-n}^{n} \|a_{n,k}\|^2 \tag{3.27}$$

is conserved between the steps of the walk and thus independent of n. Particularly,

$$S(n) = S(0) = \|a_{0,0}\|^2 = |tt^*(r^*)^{-1}|^2 = \frac{T^2}{R}, \tag{3.28}$$

where the symbols for transmittance $T = |t|^2$ and reflectivity $R = |r|^2$ of the beam splitter BS were used.

However, the symbols $a_{n,k}$ were scaled by a power of r^* in Eq. (3.23) to $\alpha(n_M, n_L)|z\rangle$. The actual probability of measuring a photon escaping in the n-th iteration of the walk ($n > 1$) is

$$C(n) = \sum_{n_M=0}^{n} \|\alpha(n_M, n - n_M)|z\rangle\|^2 = R^n S(n) = T^2 R^{n-1}. \tag{3.29 a}$$

The probability of measuring the photon in direct reflection to the detector is

$$C(0) = \|\langle\psi_o|U_{\mathrm{BS}}|\psi_i\rangle\|^2 = R. \tag{3.29 b}$$

As a verification, we note that the total probability of escaping at any iteration

$$\sum_{n=0}^{+\infty} C(n) = R + \sum_{n=1}^{\infty} T^2 R^{n-1} = R + \frac{T^2}{1-R} \tag{3.30}$$

is equal to 1 as $T + R = 1$.

3.5 Current state of experimental realization

At the time of writing this thesis, an experimental group located at Erlangen, Germany, is working on a realization of the described experiment [4] (see also the chapter introduction for additional details). In this section, we will give a brief overview of the current state of the experiment.

In order to avoid the risk of high losses and decoherence caused by a big number of reflections, the group decided to realize the long arms of the delay loop in optical fibre. However, a special polarization-maintaining fibre must be used and for best results, the PBS elements must be manufactured as in-fibre couplers. On the other hand, the fibre is made of a birefringent material and has two preferred working modes, corresponding exactly to the s and p polarization, general linear combinations obtain a nontrivial relative phase shift in this medium which can become uncontrollable over excessive optical distances. For this reason, it is necessary to couple the fibre to free space outside of the PBS–PBS delay loop to prevent polarization decoherence.

The input in the experimental realization is formed by a pulse laser at wavelength 796 nm, with the mean pulse duration of 280 fs and the repetition rate of 250 kHz. For our set of parameters, the times needed to complete one loop are $t'_M = 40$ ns and $t'_L = 45$ ns. A 50/50 beam splitter is used for the in- and out-coupling, thus $T = R = \frac{1}{2}$. An equal weight superposition is used as the initial state, produced by a sequence of a polarizing beam splitter, a half-wave plate and a quarter-wave plate applied on the laser output. The orientation of the half-wave plate HWP in Fig. 7 is easily configurable, making it possible to comparing quantum walks differing in their coin.

The testing measurements of the individual optics elements have shown some additional sources of errors, some of which could be neglected and the other included in the theory. An influence of some errors on the measurement outcome is discussed in Sec. 3.7. After the main sources of errors are included in the model, the measurements show a very good agreement with the theoretical predictions up to $n = 3$. Particularly, a Hadamard walk has been arguably observed. The choice of t'_M and t'_L allows up to 8 iterations but due to the high transmittance of the beam splitter BS, the pulses are already too weak and incoherent for $n > 3$ to give useful measurement output.

3.6 Optimal layout for single photon use

Using the same approach as in Sec. 2.9, we can use the transformation of single photon input state to find a response of the system on multi-photon input states, including coherent pulses. However, let us find an optimal configuration allowing the use of single photons.

The only two parts of the experiment that depend on the desired mode of operation are the light source and the detector. For single photons, an avalanche photodiode (APD)-based detector must be used [19]. Its principle of operation makes it much more sensitive than a pulse detector but also much more vulnerable. One must take serious care that a non-attenuated pulse never reaches the detector in operational mode.

As far as the input is concerned, the group decided to use a highly attenuated pulse laser output. If we approximate the pulses produced by the laser by coherent states (or a superposition of them), the attenuation reduces the absolute value of their amplitude. However, the probability distribution of the photon number stays Poissonian, which is the result for any coherent state (see App. A). Thus, in order to reduce the probability of measuring multi-photon states as much as possible, the mean photon number in the pulse is usually attenuated as much as several orders of magnitude below 1. Only a few of the pulses will actually initialize a successful run of the experiment.

In order to get more useful data from the experiment, we will aim for measuring as high iteration counts as possible. For this purpose, it is necessary to reduce the exponential decay of probability per one iteration. According to Eq. (3.29 a), the decay will be less when the reflectivity R of the beam splitter BS increases. On the other hand, R also determines the probability of trivial result in Eq. (3.29 b), so if it is close to 1, nearly every input photon is observed in the detector directly and not coupled into the interferometer at all. This further reduces the rate of successful runs.

One could make the input pulse stronger and make this filter at the in-coupling beam splitter a part of the pulse attenuation chain. However, one would risk a damage of the single photon detector by the reflected part of the pulse under such arrangement. One way would be to screen this pulse out and start the detection afterwards. Another solution of this problem can be reached by using two beam splitters, one solely for the purpose of in-coupling and the other one for out-coupling, both configured so that there is nearly unit probability to stay inside the interferometer. In this way, one can avoid the risk of damaging the detector without the need for a $t'_{M,L}$-timescale controllable protective screen.

3.7 Imperfections and decoherence

Experimental data show various differences to the ideal behaviour of the optical elements, described above. Let us list the main sources of errors in this section.

First, let us concentrate on losses in the experiment. The measurements in [4] have shown that the losses at the PBS–PBS loop, for example, are over 50 % in addition to the 50 % of intensity out-coupled at BS at every loop. Moreover, the losses are very different for the s- and p-polarization states in favour of the s-polarization.

In order to include these losses in the description, we can define an additional operator on the state which reduces the amplitudes of the distinct polarization components accordingly,

$$L = \lambda_s |s\rangle\langle s| + \lambda_p |p\rangle\langle p|, \tag{3.31}$$

and apply it on the polarization state right after the action of the half-wave plate HWP. By defining

$$\tilde{U} = L U_{\mathrm{HWP}}, \tag{3.32}$$

the losses can be included into the coin operator Eq. (3.19), introducing a generalized, non-unitary coin which can be substituted for C in all of the above formulas.

Any further losses in other parts of the interferometer can be included in the propagator analogously. For polarization-independent losses, the according "loss operator" is a multiple of the identity operator and applying it on the state can be rewritten as multiplying the state vector by a global constant factor.

Another problem is polarization mixing. It can occur by various means, including the following facts:

- the polarizing beam splitters do not separate the basis states perfectly, a small part of the improper polarization state is mixed in each output arm,
- a polarization maintaining fibre can fail to maintain the polarization state accurately when disposed to mechanical stress or when used for excessively long optical paths,
- small rotations of the mirrors incline the plane of incidence and thus mix the original s- and p-polarizations.

According to the numerical values in [4], the first two sources of errors can be neglected. The latter is not quantized in the experimental report.

In fact, if the rotations of the mirrors are uncertain or subject to thermal oscillations or other fluctuations, they cause a decoherence of the polarization state. Similarly, small uncontrolled spatial shifts of the mirrors cause a decoherence in the position space. As decoherence in quantum walks is a very broad topic, discussed extensively e.g. in [29], we will only demonstrate the effects of polarization decoherence on a simplified example here.

Let us consider the interaction of a polarized beam with a mirror. Let the incident beam be in a pure polarization state, described by a state vector

$$|\psi_i\rangle = \alpha|p\rangle + \beta|s\rangle = \begin{pmatrix} \alpha \\ \beta \end{pmatrix}, \tag{3.33}$$

where the $|p\rangle$ and $|s\rangle$ kets are determined geometrically by other parts of the experiment. The right hand side is a column expansion of the vector in this basis. Let the mirror is tilted slightly such that the plane of incidence differs from the plane defining the preferred basis of $\mathcal{H}_C$. As a result, let us assume that the polarization state of the reflected beam is rotated due to the polarization state of the incident beam by an angle of φ, that is,

$$|\psi_o\rangle = \begin{pmatrix} \cos\varphi & -\sin\varphi \\ \sin\varphi & \cos\varphi \end{pmatrix} \begin{pmatrix} \alpha \\ \beta \end{pmatrix} = R(\varphi)|\psi_i\rangle. \tag{3.34}$$

If the angle φ is unknown and given only by a probability distribution, we will show that the pure state $|\psi_i\rangle\langle\psi_i|$ is generally transformed to a mixed state, which is the origin of the decoherence. Let us assume that the distribution of the possible angles $\varphi \in \mathbb{R}$ is Gaussian,

$$w(\varphi) = \frac{1}{\sqrt{2\pi\sigma^2}} e^{-\frac{\varphi^2}{2\sigma^2}}. \tag{3.35}$$

The polarization state of the reflected beam is found as an integral of

$$\varrho_o = \int_{\mathbb{R}} |\psi_o\rangle\langle\psi_o| w(\varphi)\mathrm{d}\varphi = \int_{\mathbb{R}} R|\psi_i\rangle\langle\psi_i|R^\dagger w(\varphi)\mathrm{d}\varphi. \tag{3.36}$$

Let

$$\varrho_i = |\psi_i\rangle\langle\psi_i| = \begin{pmatrix} \varrho_{11} & \varrho_{12} \\ \varrho_{12} & \varrho_{22} \end{pmatrix} = \begin{pmatrix} |\alpha|^2 & \alpha\beta^* \\ \beta\alpha^* & |\beta|^2 \end{pmatrix} \tag{3.37}$$

be the initial pure state. After expanding the matrix product in Eq. (3.36), the state ϱ_o can be written as

$$\varrho_o = \begin{pmatrix} \tilde{\varrho}_{11} & \tilde{\varrho}_{12} \\ \tilde{\varrho}_{21} & \tilde{\varrho}_{22} \end{pmatrix}, \tag{3.38 a}$$

where

$$\begin{aligned}
\tilde{\varrho}_{11} &= \langle\cos^2\varphi\rangle\varrho_{11} + \langle\sin^2\varphi\rangle\varrho_{22} - \langle\cos\varphi\sin\varphi\rangle(\varrho_{12} + \varrho_{21}), \\
\tilde{\varrho}_{12} &= \langle\cos^2\varphi\rangle\varrho_{12} - \langle\sin^2\varphi\rangle\varrho_{21} + \langle\cos\varphi\sin\varphi\rangle(\varrho_{11} - \varrho_{22}), \\
\tilde{\varrho}_{21} &= \langle\cos^2\varphi\rangle\varrho_{21} - \langle\sin^2\varphi\rangle\varrho_{12} + \langle\cos\varphi\sin\varphi\rangle(\varrho_{11} - \varrho_{22}), \\
\tilde{\varrho}_{22} &= \langle\cos^2\varphi\rangle\varrho_{22} + \langle\sin^2\varphi\rangle\varrho_{11} + \langle\cos\varphi\sin\varphi\rangle(\varrho_{12} + \varrho_{21}),
\end{aligned}$$

$$\langle f(\varphi)\rangle := \int_{\mathbb{R}} f(\varphi) w(\varphi)\mathrm{d}\varphi. \tag{3.38 b}$$

Using the method of contour integration, we can find the above expectation values for the probability distribution given by Eq. (3.35) to be

$$\begin{aligned}
\langle\cos^2\varphi\rangle &= \frac{1}{2}\left(1 + e^{-2\sigma^2}\right), \\
\langle\sin^2\varphi\rangle &= \frac{1}{2}\left(1 - e^{-2\sigma^2}\right), \\
\langle\cos\varphi\sin\varphi\rangle &= 0.
\end{aligned} \tag{3.39}$$

Plugging these values into Eq. (3.38 b), we obtain the final density matrix as

$$\varrho_o = \begin{pmatrix} \frac{1}{2} + \frac{1}{2}e^{-2\sigma^2}(\varrho_{11} - \varrho_{22}) & \frac{1}{2}(\varrho_{12} - \varrho_{21}) + \frac{1}{2}e^{-2\sigma^2}(\varrho_{12} + \varrho_{21}) \\ \frac{1}{2}(\varrho_{21} - \varrho_{12}) + \frac{1}{2}e^{-2\sigma^2}(\varrho_{12} + \varrho_{21}) & \frac{1}{2} + \frac{1}{2}e^{-2\sigma^2}(\varrho_{22} - \varrho_{11}) \end{pmatrix}. \tag{3.40}$$

For $\sigma = 0$, ϱ_o becomes ϱ_i as expected. However, when there is some nonzero variance of the angle φ, ϱ_o is a mixed state except for some specially chosen cases of ϱ_i. We can prove this by computing the trace of ϱ_o^2:

$$\begin{aligned}
\mathrm{Tr}\,\varrho_o^2 &= \frac{1}{2}\left(1 - (\varrho_{12} - \varrho_{21})^2 + \left((\varrho_{11} - \varrho_{22})^2 + (\varrho_{12} + \varrho_{21})^2\right) e^{-2\sigma^2}\right) = \\
&= \frac{1}{2}\left(1 + 4\varrho_{12}\varrho_{21} + (\varrho_{11} - \varrho_{22})^2 + \left((\varrho_{11} - \varrho_{22})^2 + (\varrho_{12} + \varrho_{21})^2\right)(e^{-2\sigma^2} - 1)\right) = \\
&= \frac{1}{2}\left(a + b(e^{-2\sigma^2} - 1)\right).
\end{aligned} \tag{3.41}$$

Using the relation that

$$\operatorname{Tr} \varrho_i = \operatorname{Tr} \varrho_i^2 = 1, \tag{3.42}$$

which follows from the fact that ϱ_i is a pure state, the term a can be simplified as

$$\begin{aligned} a &= 1 + 4\varrho_{12}\varrho_{21} + (\varrho_{11} - \varrho_{22})^2 = (\varrho_{11} + \varrho_{22})^2 + (\varrho_{11} - \varrho_{22})^2 + 4\varrho_{12}\varrho_{21} = \\ &= 2\varrho_{11}^2 + 2\varrho_{22}^2 + 4\varrho_{12}\varrho_{21} = 2 \operatorname{Tr} \varrho_i^2 = 2 \end{aligned} \tag{3.43}$$

and thus

$$\operatorname{Tr} \varrho_o^2 = 1 - \frac{b}{2}(1 - e^{-2\sigma^2}). \tag{3.44}$$

Using Eq. (3.37), we can show that the coefficient b is nonnegative:

$$b = (\varrho_{11} - \varrho_{22})^2 + (\varrho_{12} + \varrho_{21})^2 = (|\alpha|^2 - |\beta|^2)^2 + (2\Re\alpha\beta^*)^2 \geq 0, \tag{3.45}$$

however, in a special case $\beta = \pm i\alpha$, it can be zero, meaning that ϱ_o is a pure state for any σ. This special case was allowed by restricting the unitary transform in Eq. (3.34) to one degree of freedom only. If we allowed more general unitary transforms, the decoherence would be even stronger.

3.8 Summary

In this chapter, a system depicted in Fig. 7 was studied. The mathematical model showed that it is a very straightforward implementation of a coined discrete time quantum walk on a line described by many authors in the references. Therefore, any result from there should have a direct representation in this system.

The reconstruction of the quantum walk from the experiment's output is done the same way as in Chap. 2, however, it was shown that probability renormalization of the time bins is done by multiplying them by a simple expression exponential in the iteration count.

The implementation discussed in this chapter is currently realized by a partner experimental group. The current state of this experiment was presented as well as some numerical data about this particular realization. Also, an optimization approach for single photon use was proposed which could be used in a future version of the experiment.

Chapter 4
Quantum walk using a diffraction grating

In this chapter, we will present and discuss another simple implementation of a quantum walk using the principle of diffraction on an optical grating.

4.1 The properties of diffraction grating

To describe the action of an optical grating as a linear optics element, we will revert to wave optics. The reason is that due to the complicated interaction of the light and the grating, the principles of quantum electrodynamics (QED) would have to be used, which is outside the scope of this work. The Huygens-Fresnel principle, used below, is a classical, phenomenological version of the quantum path integral and a sufficient replacement for our purposes.

Let a diffraction grating have N slits separated by a and each of width d. Let a monochromatic plane wave be incident on the grating at an angle of ψ such that the projection of its wave vector $\vec{k}$ onto the plane of the grating is orthogonal to the slits. Let us define a two-dimensional polar coordinate system (r, φ) in the plane of incidence, where the angle φ is measured from the normal to the grating. The above parameters and the coordinate system are depicted in Fig. 9. Assuming that the slits length is much larger than a, the problem has an approximate translation symmetry in the third orthogonal axis, which justifies the use of two-dimensional description.

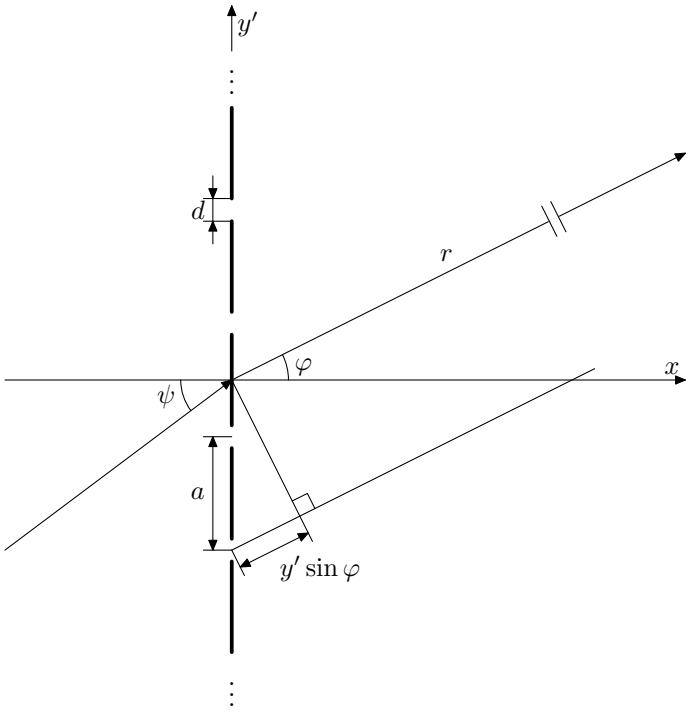

Fig. 9: A zoom of a diffraction grating. Various notation used in the text is visualized. Both the incident and diffracted plane waves are depicted.

According to the Huygens–Fresnel principle [30], we get the amplitude of the diffracted wave at the coordinates (r, φ) in the far-zone as an integral of infinitesimal contributions of point sources distributed along the transparent parts of the grating. If the angle $\psi = 0$, these sources are all in phase, otherwise their relative phase is linear in their y-coordinate with the factor of $k_y^{\text{inc.}} = -k \sin \psi$. Using the notation of Fig. 9, the amplitude is computed as

$$\alpha(r, \varphi) = A(r) K(\psi, \varphi) e^{-ikr} \int_{\text{aperture}} e^{(-ik \sin \psi + ik \sin \varphi) y'} \mathrm{d}y', \tag{4.1}$$

where $A(r)$ is a normalization factor and K is an *inclination factor* dependent on the angle of diffraction, $|\psi - \varphi|$. We will assume that K is normalized to 1 for $\psi = \varphi$. The dependence of A on the geometrical parameters N, d and a is also noted but not explicitly written. Defining

$$\sigma = \sin \varphi - \sin \psi \tag{4.2}$$

and introducing the particular shape of the aperture, the integral can be rewritten to

$$\alpha(r, \varphi) = A(r) K(\psi, \varphi) e^{-ikr} \sum_{j=1}^{N} \int_{y'_j - \frac{d}{2}}^{y'_j + \frac{d}{2}} e^{ik\sigma z} \mathrm{d}z, \tag{4.3 a}$$

where

$$y'_j = \left(j - \frac{N+1}{2} \right) a. \tag{4.3 b}$$

After computing the auxiliary integral

$$\int_{y'_j - \frac{d}{2}}^{y'_j + \frac{d}{2}} e^{ik\sigma z} \mathrm{d}z = e^{ik\sigma y'_j} \int_{-\frac{d}{2}}^{\frac{d}{2}} e^{ik\sigma z'} \mathrm{d}z' = e^{ik\sigma y'_j} \int_{-\frac{d}{2}}^{\frac{d}{2}} \cos k\sigma z' \mathrm{d}z' = \frac{2 e^{ik\sigma y'_j}}{k\sigma} \sin \frac{k\sigma d}{2}, \tag{4.4}$$

we can sum Eq. (4.3 a) as

$$\begin{aligned}
\alpha(r, \varphi) &= A(r) K(\psi, \varphi) e^{-ikr} \cdot \frac{2 \sin \frac{k\sigma d}{2}}{k\sigma} \sum_{j=1}^{N} e^{ik\sigma y'_j} = \\
&= A(r) K(\psi, \varphi) e^{-ikr} \cdot \frac{2 \sin \frac{k\sigma d}{2}}{k\sigma} \sum_{j=1}^{N} e^{ik\sigma \left(j - \frac{N+1}{2} \right) a} = \\
&= A(r) K(\psi, \varphi) e^{-ikr} \cdot \frac{2 \sin \frac{k\sigma d}{2}}{k\sigma} e^{-ik\sigma \frac{N+1}{2} a} \sum_{j=1}^{N} e^{ik\sigma j a} = \\
&= A(r) K(\psi, \varphi) e^{-ikr} \cdot \frac{2 \sin \frac{k\sigma d}{2}}{k\sigma} e^{-ik\sigma \frac{N+1}{2} a} \cdot \frac{e^{ik\sigma (N+1) a} - e^{ik\sigma a}}{e^{ik\sigma a} - 1} = \\
&= A(r) K(\psi, \varphi) e^{-ikr} \cdot \frac{2 \sin \frac{k\sigma d}{2}}{k\sigma} \cdot \frac{e^{ik\sigma \frac{N}{2} a} - e^{-ik\sigma \frac{N}{2} a}}{e^{ik\sigma \frac{a}{2}} - e^{-ik\sigma \frac{a}{2}}} = \\
&= A(r) e^{-ikr} \cdot \frac{2 \sin \frac{k\sigma d}{2}}{k\sigma} \cdot \frac{\sin k\sigma \frac{N}{2} a}{\sin k\sigma \frac{a}{2}} K(\psi, \varphi).
\end{aligned} \tag{4.5}$$

This equation splits into three significant terms:

- a term indicating a cylindrical wave propagating from the axis of symmetry of the grating perpendicular to the plane of incidence,
- an envelope function given by the nonzero width of the slits,
- a directional characteristic function, independent of r and d.

We also note that Eq. (4.5) is undefined for a finite subset of possible values of σ but can be continuously extended to cover these points.

Analyzing these terms, we find that if the slits are narrow enough, namely for

$$d \leq \frac{\pi}{2k}, \tag{4.6}$$

the "envelope" term varies so slowly that it never reaches zero for any choice of ψ and φ. For an idealized grating with infinitely narrow slits, it approaches a constant in σ but on the other hand, only an infinitesimal part of the incident wave is actually diffracted.

The last term is typical for diffraction gratings: aside from the inclination factor, it is a periodic function of σ (restricted to an interval reachable by Eq. (4.2)), reaching *major maxima* of N for

$$\sigma = m\frac{2\pi}{ka}, \quad m \in \mathbb{Z}. \tag{4.7}$$

Between each adjacent pair of major maxima, there are $N-2$ unequally separated *minor maxima* in the absolute value. For large N, most intensity of the diffracted light is concentrated near the angles φ corresponding to major maxima, the other peaks are suppressed.

4.2 Diffraction grating as a linear optics element

The previous section can be summarized as follows: when a plane wave is incident on a diffraction grating with a large number of narrow slits, it is diffracted into a finite number of narrow angle ranges (in a projection onto the plane of incidence) with nearly equally distributed intensities. If we replace the plane wave by a beam, the diffraction grating transforms it into several output beams in the plane of incidence. To justify the calculations exactly, we must add to the assumptions that only a relative part of the slit count, $\tilde{N}$, proportional to the mean width of the beam, is considered, and it is still much greater than 1.

If the angle of incidence is ψ, the angles of the outgoing beams, φ_m, are given by

$$\sin\varphi_m - \sin\psi = m\frac{2\pi}{ka}, \quad m \in \mathbb{Z}, \tag{4.8 a}$$

together with the inequality

$$-\frac{\pi}{2} \leq \varphi_m \leq \frac{\pi}{2}. \tag{4.8 b}$$

There is always a trivial solution $\varphi_0 = \psi$. Let us assume that there is another solution, φ_n. Note that if another beam is incident at the angle of φ_n, the set of solutions is the same—therefore,

the diffraction grating can act similarly to a multiport, mixing input beams incident at one spot at angles $\{\varphi_m\}$ in output beams under the same set of angles. However, due to the losses and interaction with the material, the transformation is not unitary. Also, the divergence of the output beams, given by the nonzero width of the peaks of Eq. (4.5), can be a problem for larger scale use.

For our purposes, we will need to minimize the number of the multiport channels. From Eq. (4.8 a), we can note that the sines of φ_m are equidistant, they must naturally also be bounded inside the interval $\langle -1, 1\rangle$. For given ψ, this gives an inequality for m,

$$(-1 - \sin\psi)\frac{ka}{2\pi} \leq m \leq (1 - \sin\psi)\frac{ka}{2\pi}, \tag{4.9}$$

which has

$$n_m = \left\lfloor (1 - \sin\psi)\frac{ka}{2\pi} \right\rfloor + \left\lfloor (1 + \sin\psi)\frac{ka}{2\pi} \right\rfloor + 1 \tag{4.10}$$

solutions in $\mathbb{Z}$.

If we restrict ourselves to $\psi = 0$, there is always an odd number of output beams. The case $n_m = 1$ is trivial: the beam is mostly transmitted by the grating with only the negative effects mentioned above. Thus we can say that the nontrivial minimum is 3. In order to reach 3 clearly distinguishable output modes, we can put the inner of the whole part to be 1.5:

$$\begin{aligned} \frac{ka}{2\pi} &= \frac{3}{2}, \\ a &= \frac{3\pi}{k}. \end{aligned} \tag{4.11}$$

In terms of the wavelength,

$$\lambda = \frac{2\pi}{k}, \tag{4.12}$$

the condition is $a = \frac{3}{2}\lambda$. The output modes are obtained by solving Eq. (4.8 a) for $m = 0$ (zeroth order maximum) and $m = \pm 1$ (first order maxima) with the restriction of Eq. (4.8 b), giving

$$\varphi_0 = 0, \quad \varphi_{\pm 1} = \pm \arcsin\frac{2}{3} \approx \pm 0.232\pi. \tag{4.13}$$

Without the restriction that one mode is perpendicular to the grating, we can reach a two-mode operation, resembling a beam splitter. We can find the corresponding a similarly as above, solving a system

$$\begin{aligned} (1 - \sin\psi)\frac{ka}{2\pi} &= \frac{1}{2}, \\ (1 + \sin\psi)\frac{ka}{2\pi} &= \frac{3}{2}. \end{aligned} \tag{4.14}$$

This system gives values for both a and ψ:

$$\begin{aligned} a &= \frac{2\pi}{k} = \lambda, \\ \psi &= \arcsin\frac{1}{2} = \frac{\pi}{6}. \end{aligned} \tag{4.15}$$

Let us find the transfer matrix in both cases, that is, the matrix transforming the tuple of input beam amplitudes to the tuple of output beam amplitudes. In order to find it, we will plug every combination of the input and output angles into Eq. (4.2) and use these results for taking a limit of Eq. (4.5). For dimensionality purposes, we can divide the matrix elements by the measure of the aperture, Nd. Also, we will drop the first term of Eq. (4.5) out of the matrix as it describes the behaviour outside the grating and not the transformation itself. With these modifications, one matrix element is reduced to

$$\frac{2}{k\sigma d}\sin\frac{k\sigma d}{2}K(\psi,\varphi). \tag{4.16}$$

In the 3-mode case, the first, second and third component of the amplitude vector will correspond to the beams in the directions of φ_-, φ_0 and φ_+, in this order. Using Eq. (4.16), we find the transfer matrix as

$$T=\begin{pmatrix}1 & u & v\\ u & 1 & u\\ v & u & 1\end{pmatrix}, \tag{4.17 a}$$

where

$$u=\frac{3}{kd}\sin\frac{kd}{3}K(0,\varphi_+),\quad v=\frac{3}{2kd}\sin\frac{2kd}{3}K(\varphi_-,\varphi_+). \tag{4.17 b}$$

We emphasize that this matrix is generally not unitary.

For the 2-mode operation, the transformation is similar,

$$\begin{aligned}T&=\begin{pmatrix}1 & v\\ v & 1\end{pmatrix},\\ v&=\frac{2}{kd}\sin\frac{kd}{2}K(\varphi_-,\varphi_+).\end{aligned} \tag{4.18}$$

Note that the transfer matrix is strongly dependent on the width of the diffraction grating slits, d. For this reason, the grating can not be idealized.

4.3 Quantum walk with a line of diffraction gratings

Let us try to exploit the properties of a diffraction grating to implement a quantum walk scenario. The calculations done in Sec. 4.2 are not quantum but their results contain information about both absolute value of amplitude and phase of the diffracted beams. Using this, we can build a semi-quantum mathematical approach, as shown below.

The proposed experimental configuration is depicted in Fig. 10. A line of identical diffraction gratings is aligned parallel to each other and spaced equally. The distance of two neighbouring gratings, b, must be large enough for the far-zone approximation to be used. As discussed in Sec. 4.2, the waves will propagate in a fixed number of preferred directions between each pair of adjacent gratings, also, it follows that the beams will meet at n *nodes* on the n-th grating, if counted from the left. All paths leading to a given node have the same mean path length, which guarantees good interference.

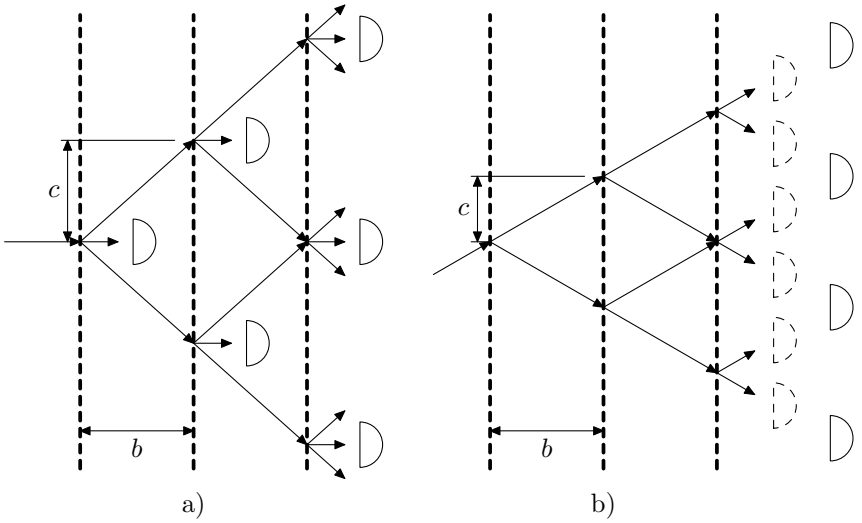

Fig. 10: The third configuration to be studied. The use of three-mode and two-mode configuration (a and b, respectively) for a Quincunx-like operation is depicted. Note that the actual behaviour does not depend only on the angle of incidence of the input beam but also on the ratio of the grating constant a to the wavelength. The image b) gives two different possibilities of where to place the output detectors.

We will assume that the relation between the wavelength and the parameter a and the input angle ψ are chosen such that the diffraction grating defines 3 or 2 modes, as described in Sec. 4.2. In the former case, we will place a detector measuring the middle beam behind each node, leaving only two beams propagating to the next grating. Alternatively, we can screen the middle beams out. We let the light waves in the two-mode case propagate freely.

In both cases, the beams connecting the nodes form a grid structure strongly resembling a random walk. However, in the following, we will show that the behaviour of the system is even closer to a quantum walk, as described in Sec. 1.1.

Let us denote the nodes in Fig. 10 by pairs of numbers as follows: let n denote the zero-based index of the diffraction grating, counted from the left. Thus the leftmost diffraction grating will correspond to $n = 0$, the next one to $n = 1$, etc. Let m denote the vertical coordinate in the figure, counted in the units of c. Let the normal at the first point of incidence define the axis where $m = 0$. It then follows from the layout that m is integer for each node and that it is bounded by the following two conditions,

$$\begin{aligned} -n \leq m \leq n, \\ m \equiv n \pmod 2. \end{aligned} \tag{4.19}$$

These conditions are the same as the conditions where the probability of a particle performing a random walk or a quantum walk on a line can be nonzero if n denotes the iteration count and m the position and the walk starts at $m = 0$. For this reason, let us identify the n and m parameters with these physical values.

Let us describe the system's behaviour in a similar manner to Sec. 1.1. We note that we do not attempt to build a quantum description, we just write the above results in an algebraical way, reusing the symbol names from Sec. 1.1.

First, let us define two complex vector spaces, $\mathcal{H}_S$ of countably infinite dimension and $\mathcal{H}_C$ of dimension 2. Let there be a basis of $\mathcal{H}_S$ denoted $\{|x\rangle \mid x \in \mathbb{Z}\}$ and a basis of $\mathcal{H}_C$ denoted $\{|L\rangle, |R\rangle\}$. Let us find a vector space $\mathcal{H}$ as a tensor product $\mathcal{H} = \mathcal{H}_S \otimes \mathcal{H}_C$. We can find a basis of $\mathcal{H}$ as a tensor product of the two bases using Eq. (1.1).

For a fixed n, we can build a vector in this space describing the beams incident on the diffraction grating with index n: let $a_\pm(n, m)$ is the amplitude, including relative phase, of the beam incident at the node with coordinate m and coming from the positive or negative relative m from the previous diffraction grating. Using these amplitudes, we can define an unnormalized vector $v_n \in \mathcal{H}$ as

$$v_n = \sum_{m \in \mathbb{Z}} \left(a_{m,-} |m, R\rangle + a_{m,+} |m, L\rangle \right). \tag{4.20}$$

This definition is correct since only a finite number of the coefficients $a_{m,\pm}$ can be nonzero.

The propagation from the n-th to the $(n + 1)$-th diffraction grating can be described as an action of three operators: first, the beams are diffracted and transformed by the transfer matrix, after which they are spatially separated by passing the distance b. Finally, a partial absorption of the beams is counted in before the next iteration.

The transformation induced by diffraction can be described by an operator

$$C = \mathbb{1} \otimes C_0, \tag{4.21}$$

acting on $\mathcal{H}_C$ only. The operator C_0 will be defined using its matrix in the $\{|L\rangle, |R\rangle\}$ basis, which is equal to the transfer matrix Eq. (4.18) in the 2-mode operation. In the 3-mode configuration, the unused middle beam must be projected out by restricting the matrix Eq. (4.17 a) to the first and third component only. In this restriction, it obtains formally the same shape as Eq. (4.18), but with the v parameter given by Eq. (4.17 b).

The propagation in free space is described by the operator

$$S = A(r) e^{-ikr} \sum_{m \in \mathbb{Z}} \left(|m + 1, R\rangle\langle m, R| + |m - 1, L\rangle\langle m, L| \right), \tag{4.22}$$

where the factor $A(r) \exp(-ikr)$ comes from Eq. (4.5) and r is the distance travelled by the beam,

$$r = \sqrt{b^2 + c^2}. \tag{4.23}$$

The symbols $\langle m, R|$ and $\langle m, L|$ are the coordinate functionals of the basis vectors $|m, R\rangle$ and $|m, L\rangle$, respectively. For finite linear combinations, which form the linear span, the coordinate functionals are well-defined. Also, Eq. (4.22) maps finite linear combinations of the basis vectors to other finite linear combinations of these and so it preserves $\mathcal{H}$.

Finally, the losses between two iterations can be modelled by multiplicating the vector by a real constant, q.

Putting these three transformations together, the relation between the situation at two subsequent diffraction gratings can be described by the equation

$$v_{n+1} = qSCv_n, \tag{4.24}$$

which is, up to a constant of $qA(r)\exp(-ikr)$, equivalent to Eq. (1.3 a) with a special choice of C, described above. The constant factor can be included into the operator C, after which the usual methods of solving or simulations, designed for unitary quantum walks, can be used with little or no changes.

The initial state of the walk can be described in a straightforward way as the vector v_0 if the initial beam is incident on the first grating at one of the nonzero preferred angles to the normal. An example of this situation is shown in Fig. 10 b). On the other hand, if the input beam is parallel with the normal, which can be the case in the 3-mode variant, the first iteration must be computed by hand and the initial condition must be given in the form of v_1. According to Eqs. (4.24) and (4.17 a), the initial condition in this case is

$$v_1 = quA(r)e^{-ikr}(|1,R\rangle + |-1,L\rangle). \tag{4.25}$$

4.4 Measurement of the walk

Due to the spatial separation of the nodes, measuring of the magnitude of the components of v_n is straightforward. According to Fig. 10 b), we can place a line of detectors at the location where the nodes of the grating with index n would be. Alternatively, one detector can be used for each individual mode if desired. This approach can be used for both experimental scenarios.

In the case of the 3-mode operation, we can use detectors shown in Fig. 10 a) to measure the middle output mode of each node in addition to, or instead of, the distribution after n steps as described above. However, the meaning of the intensity of these beams needs some explanation.

Let the next to the last state vector, v_{n-1}, be written as

$$v_{n-1} = \sum_{m=1-n}^{n-1} (a_{m,-}|m,R\rangle + a_{m,+}|m,L\rangle). \tag{4.26}$$

The beams incident at the node at coordinate m can be written, in the sense of Eq. (4.17 a), as a 3-component vector

$$v = \begin{pmatrix} a_{m,-} \\ 0 \\ a_{m,+} \end{pmatrix}. \tag{4.27}$$

The diffraction grating transforms it into

$$Tv = \begin{pmatrix} a_{m,-} + va_{m,+} \\ u(a_{m,-} + a_{m,+}) \\ a_{m,+} + va_{m,-} \end{pmatrix}, \tag{4.28}$$

so that the amplitude of the middle output beam is proportional to the *sum* of amplitudes of the two incident beams. In other words, the intensity measured at the detector is a result of interference of these two beams.

4.5 Summary

In this chapter, a basic study of the possibilities of implementing a quantum-like walk using a diffraction grating was provided. First, the formula for diffraction on a grating was carefully derived and studied. It was shown that under some assumptions, a diffraction grating can behave similarly to an optical multiport acting in free space. This fact makes it a new element available for use in optical interferometers.

A configuration using a line of identical diffraction gratings in order to implement a random walk scenario was studied. This idea differs significantly from the principle used in the previous two chapters, one of the most striking differences is that the space requirements scale quadratically in the maximal number of steps wanted to be performed.

Despite the fact that the treatment of the diffraction grating was classical, the resulting formulae resemble strongly the quantum walk introduced in Sec. 1.1. For this reason, the result could be called a generalized quantum walk with non-unitary coin.

Conclusion

Quantum walks have become an active field of research, in particular in connection to quantum algorithms, during the last decade. Several important algorithmic tasks have also been solved using quantum algorithms based on quantum walks. As the theory of quantum walks is already very rich, a demand naturally arises to find a flexible experimental implementation. A realization allowing various changes to the basic quantum walk would be a significant step towards a quantum computer since its framework could allow direct realization of some of the quantum walk-based algorithms.

There are many ways of implementing quantum algorithms in general. In this thesis, we studied the possibilities of implementing a quantum walk using an optical interferometer. One of the configurations proved to have a very close relation to the basic coined discrete-time quantum walk on a line and thus offers a possible way to pursue this line also in subsequent work. The other configurations feature some generalized forms of quantum walks, which have not been studied so far and thus their potential is not yet completely explored.

As noted in the introduction and in the respective places, some parts of the work were collaborative. However, most of the work of the original results presented in Chapters 2 to 4 have been the author's work within the presented Master's thesis. Naturally, the experiments discussed are completely the work of the colleagues in Erlangen.

The work done here opens some opportunities for a subsequent research. The next important step would be to find a realization of some simple quantum algorithm based on one of the presented implementations. Another significant open question is how more complicated quantum walks, e.g., a walk on a 2-dimensional lattice instead of a line, could be implemented in a similar manner. Work on these topics is well under way and we expect our partners from Erlangen to catch on these ideas in near future.

Appendix A
Coherent states

Coherent states form an important subset of the state space of an electromagnetic field. In this Appendix, we will define these states and study some of their properties.

A.1 The ladder operators

Let us begin with introducing the Hamiltonian of a quantum harmonic oscillator from elementary quantum mechanics [31],

$$H = \frac{1}{2}X^2 + \frac{1}{2}P^2. \tag{A.1}$$

The X and P operators are the position and momentum observables in a set of units where the mass of the particle, the angular frequency of the oscillator and the reduced Planck constant $\hbar$ are all equal to 1, and satisfy a canonical commutation relation

$$[X, P] = i. \tag{A.2}$$

In quantum optics, the same Hamiltonian describes the dynamics of every mode of an electromagnetic field [27]. The X and P observables lose their original direct meaning but are still observable quantities subsequently referred to as *quadratures* of the mode.

Similarly to a harmonic oscillator, any mode of an electromagnetic field has a nondegenerate state with a lowest energy, the *vacuum state* $|0\rangle$. It can be shown that the spectrum of H is discrete and all the eigenstates can be generated from $|0\rangle$ using so called *ladder operators*.

Definition 1: A *ladder operator* (with respect to another operator H) is any operator A which satisfies the commutation relation

$$[H, A] = \alpha A, \tag{A.3}$$

where $\alpha \in \mathbb{C}$.

The importance of such operators follows from the following Lemma.

Lemma 2: Let $\alpha \in \mathbb{C}$, let H and A be two operators such that $[H, A] = \alpha A$. Let further $|\psi\rangle$ be an eigenvector of H with eigenvalue λ, that is,

$$H|\psi\rangle = \lambda|\psi\rangle. \tag{A.4}$$

Then

$$HA|\psi\rangle = (\lambda + \alpha)A|\psi\rangle, \tag{A.5}$$

i.e., $A|\psi\rangle$ is either a zero vector or an eigenvector of H with eigenvalue $\lambda + \alpha$.

Proof: Let us expand the commutation relation

$$[H, A] = HA - AH = \alpha A \tag{A.6}$$

and apply both sides on $|\psi\rangle$. After rewriting,

$$HA|\psi\rangle = AH|\psi\rangle + \alpha A|\psi\rangle. \tag{A.7}$$

Using Eq. (A.4) and the linearity,

$$HA|\psi\rangle = \lambda A|\psi\rangle + \alpha A|\psi\rangle = (\lambda + \alpha)A|\psi\rangle. \tag{A.8}$$

■

Let us try to find ladder operators of H as linear combinations of X and P. From Eqs. (A.1) and (A.2), it can be directly shown that

$$[H, X] = -iP \quad \text{and} \quad [H, P] = iX, \tag{A.9}$$

thus

$$[H, \alpha X + \beta P] = i(\beta X - \alpha P). \tag{A.10}$$

If we equate the right hand side to $\lambda(\alpha X + \beta P)$, we can find the following two solutions:

$$\beta = \pm\alpha \quad \text{for} \quad \lambda = \mp 1. \tag{A.11}$$

Letting α a fixed real number, we obtain two mutually adjoint operators, shifting the eigenvalues of (A.1) by ± 1. Especially, for $\alpha = 1/\sqrt{2}$, these operators are called the *annihilation operator* a and the *creation operator* $a^\dagger$:

$$\begin{aligned} a &= \frac{1}{\sqrt{2}}(X + iP), \\ a^\dagger &= \frac{1}{\sqrt{2}}(X - iP). \end{aligned} \tag{A.12}$$

The reason for choosing α in this particular way is that in this case, a and $a^\dagger$ follow a simple commutation relation

$$[a, a^\dagger] = 1/2[X + iP, X - iP] = 2\frac{i}{2}[P, X] = 1. \tag{A.13}$$

The relations (A.12) can be inverted to express X and P in terms of a and $a^\dagger$,

$$\begin{aligned} X &= \frac{1}{\sqrt{2}}(a + a^\dagger), \\ P &= -\frac{i}{\sqrt{2}}(a - a^\dagger), \end{aligned} \tag{A.14}$$

allowing us to express H only in terms of the ladder operators:

$$H = \frac{1}{2}\{a, a^\dagger\} = \frac{1}{2}(aa^\dagger + a^\dagger a) = \frac{1}{2}(2a^\dagger a + [a, a^\dagger]) = a^\dagger a + \frac{1}{2}. \tag{A.15}$$

As $|0\rangle$ is the lowest energy state, $a|0\rangle$ is necessarily the zero vector. In the units we have been using, this implies that

$$H|0\rangle = \frac{1}{2}. \tag{A.16}$$

On the other hand, we can apply the creation operator or any positive power of it on $|0\rangle$ to obtain eigenstates of H with eigenvalues $n+\frac{1}{2}$ for any $n \in \mathbb{N}_0$. Applying a ladder operator several number of times could generally end in the zero vector—however, we will quickly show that this does not happen with $a^\dagger$ applied on $|0\rangle$.

For this purpose, we will derive from Eq. (A.12) the identity

$$a(a^\dagger)^n = n(a^\dagger)^{n-1} + (a^\dagger)^n a. \tag{A.17}$$

Let us study the norm of $(a^\dagger)^n|0\rangle$, applying this result:

$$\begin{aligned} \|(a^\dagger)^n|0\rangle\|^2 &= \langle 0|a^n(a^\dagger)^n|0\rangle = \langle 0|a^{n-1}\left(n(a^\dagger)^{n-1} + (a^\dagger)^n a\right)|0\rangle = \\ &= n\langle 0|a^{n-1}(a^\dagger)^{n-1}|0\rangle + 0 = n\left\|(a^\dagger)^{n-1}|0\rangle\right\| = \\ &= n(n-1)\left\|(a^\dagger)^{n-2}|0\rangle\right\| = \ldots = n!\||0\rangle\| = \\ &= n!. \end{aligned} \tag{A.18}$$

We see that the norm is nonzero for any $n \in \mathbb{N}_0$. Therefore, we can define normalized *number states*

$$|n\rangle = \frac{1}{\sqrt{n!}}(a^\dagger)^n|0\rangle. \tag{A.19}$$

From Eq. (A.19), we can induce the relation

$$a^\dagger|n\rangle = \sqrt{n+1}|n+1\rangle \tag{A.20 a}$$

and similarly, using Eq. (A.17),

$$a|n\rangle = \sqrt{n}|n\rangle. \tag{A.20 b}$$

Hence, the ladder operators preserve the linear span of the number states. It follows that the existence of any other eigenvector orthogonal to this set would result in a contradiction with the nondegeneracy of the lowest energy level. Therefore, the number states form an orthonormal basis of the one-mode state space.

From the shift property Eq. (A.5) of ladder operators and from Eq. (A.16), it immediately follows that

$$H|n\rangle = \left(n + \frac{1}{2}\right)|n\rangle. \tag{A.21}$$

Comparing with Eq. (A.15), we see that the action of the operator $a^\dagger a$ on number states is simply

$$a^\dagger a|n\rangle = n|n\rangle. \tag{A.22}$$

Thus, this operator acts as a "operator of excitation count" and can be denoted accordingly by N.

A.2 The coherent states

Besides the number states, we can define many more states of general interest. The most familiar of these states are *coherent states*. We will build their definition on the above formalism. However, we note that in various sources, other definitions of coherent states than the following are also used, not necessarily compatible with the one presented here.

Definition 3: Let $\alpha \in \mathbb{C}$, let $|\psi\rangle$ be a normalized eigenvector of the annihilation operator a with eigenvalue of α. We will call $|\psi\rangle$ a *coherent state* with *amplitude* α. If $|\psi\rangle$ also satisfies a phase condition $\langle\psi|0\rangle > 0$, we will denote $|\alpha\rangle := |\psi\rangle$.

The following theorem shows that there is a coherent state for any complex amplitude α and gives a formula how to find it.

Theorem 4: Let $\alpha \in \mathbb{C}$, let $|0\rangle$ be the vacuum state of the system with Hamiltonian (A.1). Then a coherent state $|\alpha\rangle$ exists and is unique. Moreover, it can be expressed in the following ways:

$$|\alpha\rangle = e^{-\frac{|\alpha|^2}{2}} \exp(\alpha a^\dagger)|0\rangle = \exp(\alpha a^\dagger - \alpha^* a)|0\rangle. \tag{A.23}$$

Proof: Let us look for the coherent state in the form

$$|\alpha\rangle = \sum_{n=0}^{+\infty} c_n |n\rangle. \tag{A.24}$$

The action of the annihilation operator is by Eq. (A.20 b)

$$a|\alpha\rangle = \sum_{n=0}^{+\infty} \sqrt{n} c_n |n-1\rangle = \sum_{n=0}^{+\infty} \sqrt{n+1}\, c_{n+1} |n\rangle. \tag{A.25}$$

Comparing this series with $\alpha|\alpha\rangle$, we obtain a recurrence relation

$$\sqrt{n+1}\, c_{n+1} = \alpha c_n \tag{A.26}$$

which can be solved as

$$c_n = \frac{\alpha^n}{\sqrt{n!}} c_0. \tag{A.27}$$

To show that this defines a state in the Hilbert space spanned by the number states, we shall show that a state defined formally by a sum

$$|\psi\rangle = c_0 \sum_{n=0}^{+\infty} \frac{\alpha^n}{\sqrt{n!}} |n\rangle \tag{A.28}$$

has a finite norm. As the number states define an orthonormal basis, the norm can be computed as

$$\||\psi\|^2 = |c_0|^2 \sum_{n=0}^{+\infty} \frac{|\alpha|^{2n}}{n!} = |c_0|^2 \exp|\alpha|^2 < +\infty. \tag{A.29}$$

Hence, we can also see that to make the state $|\psi\rangle$ normalized, the constant c_0 must satisfy

$$|c_0| = e^{-\frac{|\alpha|^2}{2}}. \tag{A.30}$$

The last, "phase" condition of Definition 3, restricts $\langle\psi|0\rangle = c_0$ to be real and positive. Thus, the state is determined uniquely:

$$|\alpha\rangle = e^{-\frac{|\alpha|^2}{2}} \sum_{n=0}^{+\infty} \frac{\alpha^n}{\sqrt{n!}}|n\rangle. \tag{A.31}$$

Using Eq. (A.19), we can rewrite Eq. (A.31) as

$$|\alpha\rangle = e^{-\frac{|\alpha|^2}{2}} \sum_{n=0}^{+\infty} \frac{\alpha^n}{n!}(a^\dagger)^n|0\rangle = e^{-\frac{|\alpha|^2}{2}} \exp(\alpha a^\dagger)|0\rangle, \tag{A.32}$$

which is exactly the first simplified form mentioned in Theorem 4.

We will prove the last equivalence in Theorem 4 indirectly by showing that the right hand side

$$|\alpha\rangle_r = \exp(\alpha a^\dagger - \alpha^* a)|0\rangle \tag{A.33}$$

satisfies all the conditions of Definition 3. First, we will find the commutation relation

$$[a, \alpha a^\dagger - \alpha^* a] = \alpha \tag{A.34}$$

and analogously to Eq. (A.17), we will prove that

$$[a, (\alpha a^\dagger - \alpha^* a)^n] = n\alpha(\alpha a^\dagger - \alpha^* a)^{n-1}. \tag{A.35}$$

Further, we will expand the exponential into a series,

$$|\alpha\rangle_r = \sum_{n=0}^{+\infty} \frac{1}{n!}(\alpha a^\dagger - \alpha^* a)^n|0\rangle. \tag{A.36}$$

Applying a from the left on both sides and using the commutation relation Eq. (A.35) and the fact that $a|0\rangle = 0$, we obtain

$$a|\alpha\rangle_r = \sum_{n=0}^{+\infty} \frac{n\alpha}{n!}(\alpha a^\dagger - \alpha^* a)^{n-1}|0\rangle = \alpha \sum_{n=1}^{+\infty} \frac{1}{(n-1)!}(\alpha a^\dagger - \alpha^* a)^{n-1}|0\rangle = \alpha|\alpha\rangle_r. \tag{A.37}$$

Next, we will show that $|\alpha\rangle_r$ is normalized. Since

$$(\alpha a^\dagger - \alpha^* a)^\dagger = \alpha^* a - \alpha a^\dagger = -(\alpha a^\dagger - \alpha^* a), \tag{A.38}$$

the operator $\alpha a^\dagger - \alpha^* a$ is skew-adjoint. Hence, its exponential is unitary and preserves the norm of $|0\rangle$ in Eq. (A.33).

Finally, we need to check the phase convention of Definition 3. Expanding the exponential again, we rewrite

$$\langle 0|\alpha\rangle_r = \sum_{n=0}^{+\infty} \frac{1}{n!}\langle 0|(\alpha a^\dagger - \alpha^* a)^n|0\rangle. \tag{A.39}$$

Using the identity that $\langle 0|a^\dagger = 0$ (since the left-hand side is a conjugate of $a|0\rangle$) and the commutation relation Eq. (A.35), we find that

$$\begin{aligned}\langle 0|(\alpha a^\dagger - \alpha^* a)^n|0\rangle &= -\alpha^*\langle 0|a(\alpha a^\dagger - \alpha^* a)^{n-1}|0\rangle = \\ &= -\alpha^*\langle 0|(\alpha a^\dagger - \alpha^* a)^{n-1}a|0\rangle - (n-1)\alpha\alpha^*\langle 0|(\alpha a^\dagger - \alpha^* a)^{n-2}|0\rangle = \\ &= -(n-1)|\alpha|^2\langle 0|(\alpha a^\dagger - \alpha^* a)^{n-2}|0\rangle.\end{aligned} \tag{A.40}$$

This recurrence relation can be solved as

$$\langle 0|(\alpha a^\dagger - \alpha^* a)^n|0\rangle = \begin{cases} (-1)^{n/2}(n-1)!!|\alpha|^n & \text{if } n \text{ is even,} \\ 0 & \text{otherwise,} \end{cases} \tag{A.41}$$

since the expression reduces for even powers of n to finding $\langle 0|0\rangle = 1$ while for odd n, it is proportional to $\langle 0|\alpha a^\dagger - \alpha^* a|0\rangle = \alpha\langle 0|1\rangle = 0$. Using this formula,

$$\begin{aligned}\langle 0|\alpha\rangle_r &= \sum_{n=0}^{+\infty} \frac{1}{n!}\langle 0|(\alpha a^\dagger - \alpha^* a)^n|0\rangle = \sum_{n=0}^{\infty} \frac{(-1)^n(2n-1)!!|a|^{2n}}{(2n)!} = \sum_{n=0}^{+\infty} \frac{(-1)^n|a|^{2n}}{(2n)!!} = \\ &= \sum_{n=0}^{+\infty} \frac{\left(-|a|^2\right)^n}{n!\,2^n} = e^{-\frac{|\alpha|^2}{2}} = \langle 0|\alpha\rangle > 0.\end{aligned} \tag{A.42}$$

This implies that $|\alpha\rangle_r = |\alpha\rangle$. ■

A.3 Basic properties of coherent states

In this section, we will list the very basic properties of coherent states. We will focus only on properties which are related to our topic in some way.

First, let us clarify the relation between number states and coherent states with integer amplitude. The vacuum state $|0\rangle$ is equal to the coherent state with amplitude 0, as can be seen e.g. from Eq. (A.32). On the other hand, number states $|n\rangle$ with $n > 0$ are *not* coherent. If a certain physical situation involves coherent states with positive integer amplitudes, the notation must be altered to avoid confusion.

As opposed to number states, no subset of coherent states can form an orthonormal basis of the state space as none of them are mutually orthogonal. Instead, the scalar product of two coherent states is

$$\langle\beta|\alpha\rangle = e^{-\frac{|\alpha|^2}{2}-\frac{|\beta|^2}{2}} \sum_{n=0}^{+\infty} \frac{\alpha^n\,(\beta^*)^n}{n!} = e^{-\frac{|\alpha|^2}{2}-\frac{|\beta|^2}{2}+\alpha\beta^*}, \tag{A.43}$$

where we used the expansion Eq. (A.31) to compute the product in the number basis. However, we note that a decomposition of unity using only coherent states is still possible in many ways, in fact, the set of coherent states is *overcomplete* [27].

Finally, we can study expectation values of the operators introduced above on coherent states. All of these can be derived algebraically from the property $a|\alpha\rangle = \alpha|\alpha\rangle$ easily:

- $\langle a\rangle_{|\alpha\rangle} = \langle\alpha|a|\alpha\rangle = \langle\alpha|\alpha|\alpha\rangle = \alpha$,
- $\langle a^\dagger\rangle_{|\alpha\rangle} = \langle\alpha|a^\dagger|\alpha\rangle = (\langle\alpha|a|\alpha\rangle)^* = \alpha^*$,
- $\langle X\rangle_{|\alpha\rangle} = \frac{1}{\sqrt{2}}(\langle a\rangle + \langle a^\dagger\rangle)_{|\alpha\rangle} = \frac{1}{\sqrt{2}}(\alpha + \alpha^*) = \sqrt{2}\Re\alpha$,
- $\langle P\rangle_{|\alpha\rangle} = \frac{-i}{\sqrt{2}}(\langle a\rangle - \langle a^\dagger\rangle)_{|\alpha\rangle} = \frac{1}{i\sqrt{2}}(\alpha - \alpha^*) = \sqrt{2}\Im\alpha$,
- $\langle N\rangle_{|\alpha\rangle} = \langle\alpha|a^\dagger a|\alpha\rangle = \||a|\alpha\rangle\|^2 = \||\alpha|\alpha\rangle\|^2 = |\alpha|^2$,
- $\langle H\rangle_{|\alpha\rangle} = \langle N\rangle_{|\alpha\rangle} + \frac{1}{2} = |\alpha|^2 + \frac{1}{2}$.

From the last two lines, we can conclude that the squared magnitude of the amplitude has a direct relation to the energy of the state. We note that the lowest energy level given by Eq. (A.16) is often subtracted from the Hamiltonian H by declaring it a zero energy level and the quantity $|\alpha|^2$ becomes proportional to the *intensity* of the pulse.

A.4 Example: a beam splitter

In this section, we will give a description of a beam splitter using the creation and annihilation operators, and use this description to compute how a coherent state input transforms on a beam splitter.

Let us begin with Eq. (2.9) from Sec. 2.3. However, instead of describing the situation for a single photon, we will define four light modes corresponding to the two input and two output arms of the beam splitter and having its own Hilbert space each. This way, we will come to a *second quantization* of the electromagnetic field: on each of the spaces, we will *postulate* the creation and annihilation operators, $a_j^\dagger$ and a_j, satisfying the canonical commutation relation Eq. (A.12), and a vacuum state $|0\rangle_j$ which satisfies $a_j|0\rangle_j = 0$. We can then reconstruct all the algebraic results of Sec. A.1. However, instead of referring to a n-th excitation of a given mode, we will claim that there are n photons in that mode, each carrying an energy of 1.

We can then identify the states used in Sec. 2.3 with tensor products of certain states of this compound system:

$$|\psi_i\rangle = |1\rangle_i \otimes |0\rangle_U \otimes |0\rangle_M \otimes |0\rangle_L = (a_i^\dagger|0\rangle_i) \otimes |0\rangle_U \otimes |0\rangle_M \otimes |0\rangle_L = a_i^\dagger|0\rangle, \tag{A.44}$$

where $|0\rangle = |0\rangle_i \otimes |0\rangle_U \otimes |0\rangle_M \otimes |0\rangle_L$ and the $a_i^\dagger$ operator is extended to act trivially on the spaces of the U, M and L modes, and, similarly,

$$\begin{aligned} |\psi_U\rangle &= a_U^\dagger|0\rangle, \\ |\psi_M\rangle &= a_M^\dagger|0\rangle, \\ |\psi_L\rangle &= a_L^\dagger|0\rangle. \end{aligned} \tag{A.45}$$

It is important to realize that the creation and annihilation operators acting on different spaces inherently commute.

Using this notation, Eq. (2.9) can be rewritten as

$$\begin{aligned} a_i^\dagger|0\rangle &\mapsto (t_A a_M^\dagger + r_A a_L^\dagger)|0\rangle, \\ a_U^\dagger|0\rangle &\mapsto (t_A^* a_L^\dagger - r_A^* a_M^\dagger)|0\rangle. \end{aligned} \tag{A.46}$$

Recall that this mapping does not happen instantaneously but takes a finite time during which the pulse travels through the beam splitter. During this time, the vacuum state can undergo some change in phase under the U_A operator. Therefore, we should correctly apply it on the vacuum state on the right hand side. In terms of this operator, the last pair of equations can be rewritten as

$$\begin{aligned} U_A a_i^\dagger|0\rangle &= (t_A a_M^\dagger + r_A a_L^\dagger)U_A|0\rangle, \\ U_A a_U^\dagger|0\rangle &= (t_A^* a_L^\dagger - r_A^* a_M^\dagger)U_A|0\rangle. \end{aligned} \tag{A.47}$$

Generally, this transition could be much more complicated, but for our purposes, we will consider an ideal passive beam splitter in constant outer conditions in which a vacuum state can only transform trivially.

In order to study the action of the beam splitter on more than one photon, we will postulate that the action is the same on each state as on the vacuum state, i.e.,

$$\begin{aligned} U_A a_i^\dagger &= (t_A a_M^\dagger + r_A a_L^\dagger)U_A, \\ U_A a_U^\dagger &= (t_A^* a_L^\dagger - r_A^* a_M^\dagger)U_A. \end{aligned} \tag{A.48}$$

Acting on both equations from the right by $U_A^\dagger$, we obtain

$$\begin{aligned} U_A a_i^\dagger U_A^\dagger &= t_A a_M^\dagger + r_A a_L^\dagger, \\ U_A a_U^\dagger U_A^\dagger &= t_A^* a_L^\dagger - r_A^* a_M^\dagger. \end{aligned} \tag{A.49}$$

We will consider this the final description of the beam splitter's action.

Taking products of powers of Eqs. (A.49) and their linear combinations, we can find the transformation of any possible input state. As an example, let us find the transformation of the input state $|1\rangle_i|1\rangle_U$ (for brevity, we omitted the tensor product operators and the kets corresponding to output states):

$$\begin{aligned} U_A a_i^\dagger a_U^\dagger U_A^\dagger = U_A a_i^\dagger U_A^\dagger U_A a_U^\dagger U_A^\dagger = (t_A a_M^\dagger + r_A a_L^\dagger)(t_A^* a_L^\dagger - r_A^* a_M^\dagger) = \\ = (T_A - R_A) a_M^\dagger a_L^\dagger - t_A r_A^* (a_M^\dagger)^2 + r_A t_A^* (a_L^\dagger)^2 \end{aligned} \tag{A.50}$$

Applying both sides of $|0\rangle$, we can see that the input state is transformed to

$$(T_A - R_A)|1\rangle_M|1\rangle_L - t_A r_A^*|2\rangle_M|0\rangle_L + r_A t_A^*|0\rangle_M|2\rangle_L, \tag{A.51}$$

which is generally an entangled state of the two output modes.

Using the same idea, we can find the action of the beam splitter when there are coherent pulses on the input modes. For this purpose, we will assume the input in the form of

$$|\alpha\rangle_i|\beta\rangle_U = e^{-\frac{|\alpha|^2+|\beta|^2}{2}} \exp(\alpha a_i^\dagger)\exp(\beta a_U^\dagger)|0\rangle = c\exp(\alpha a_i^\dagger + \beta a_U^\dagger) = c\sum_{n=0}^{+\infty} \frac{1}{n!}(\alpha a_i^\dagger + \beta a_U^\dagger)^n|0\rangle, \tag{A.52}$$

where $c = \exp((-|\alpha|^2 - |\beta|^2)/2)$ and we used the fact that $a_i^\dagger$ and $a_U^\dagger$ commute. The corresponding output state is

$$\begin{aligned}
|\psi_o\rangle &= c \sum_{n=0}^{+\infty} \frac{1}{n!} \left(U_A(\alpha a_i^\dagger + \beta a_U^\dagger) U_A^\dagger \right)^n U_A|0\rangle = \\
&= c \sum_{n=0}^{+\infty} \frac{1}{n!} (\alpha t_A a_M^\dagger + \alpha r_A a_L^\dagger + \beta t_A^* a_L^\dagger - \beta r_A^* a_M^\dagger)^n U_A|0\rangle = \\
&= c \exp(\alpha t_A a_M^\dagger + \alpha r_A a_L^\dagger + \beta t_A^* a_L^\dagger - \beta r_A^* a_M^\dagger) U_A|0\rangle = \\
&= c \exp\left((\alpha t_A - \beta r_A^*) a_M^\dagger \right) \exp\left((\alpha r_A + \beta t_A^*) a_L^\dagger \right) U_A|0\rangle = \\
&= |\alpha t_A - \beta r_A^*\rangle_M |\alpha r_A + \beta t_A^*\rangle_L,
\end{aligned} \tag{A.53}$$

where the splitting of an exponential to a product of two factors was possible since $a_M^\dagger$ and $a_L^\dagger$ commute. The normalization constant c is the same for both the input and the output state, as follows from the identity

$$\begin{aligned}
|\alpha r_A - \beta t_A^*|^2 + |\alpha r_A + \beta t_A^*|^2 &= |\alpha|^2(|t_A|^2 + |r_A|^2) + |\beta|^2(|t_A|^2 + |r_A|^2) - \\
&\quad - \alpha r_A \beta^* t_A - \beta t_A^* \alpha^* r_A^* + \alpha r_A \beta^* t_A + \beta t_A^* \alpha^* r_A^* = \\
&= |\alpha|^2 + |\beta|^2.
\end{aligned} \tag{A.54}$$

Therefore, a product of two coherent input states transforms to a product of two coherent output states, which is by definition a factorized state. This is interesting in contrast with the above two-photon case where the output was entangled. Also note in Eq. (A.53) that the amplitudes transform and "interfere" exactly in the same way as wave amplitudes in classical optics. For these reasons, coherent states are understood as the "most classical" states of light.

Appendix B
Hypergeometric sums involving two binomial coefficients

In this Appendix, we will study some properties of the series of the form

$$\sum_{m=0}^{+\infty} \binom{n-\nu_1}{m-\mu_1}\binom{n-\nu_2}{m-\mu_2} x^m, \quad \nu_1,\nu_2,\mu_1,\mu_2 \in \mathbb{N}_0, \tag{B.1}$$

which are needed at many points throughout Chap. 2. These series satisfy the condition that the ratio of two successive terms is a rational function of m and thus they form a subset of so called hypergeometric series [21]. Such series can be uniformly described using a closely related concept of hypergeometric functions [21,22]. However, as hypergeometric functions are defined again as hypergeometric series, such formal rewriting does not reduce the complexity of the calculations needed to compute the sum. Similarly, the rewriting does not give us any new information. In the following, we will keep the original series notation.

Lemma 5: Let x be a positive real number. In the series Eq. (B.1), only a finite number of terms is nonzero. These terms are consecutive and bounded by

$$\max\{\mu_1,\mu_2\} \le m \le \min\{n-\nu_1+\mu_1, n-\nu_2+\mu_2\}. \tag{B.2}$$

Proof: The binomial coefficient $\binom{n}{k}$ is zero if $k<0$ or $k>n$ and nonzero otherwise. The power term is nonzero for all m as long as x is nonzero. Applying the former rule to the two binomial coefficients in Eq. (B.1), we find that the term is zero only if and only if at least one of the conditions are met:

$$m-\mu_1<0 \text{ or } m-\mu_2<0 \text{ or } m-\mu_1>n-\nu_1 \text{ or } m-\mu_2>n-\nu_2. \tag{B.3}$$

The inverse of this condition yields the lemma. ■

As the sum for given n, μ_i and ν_i is in fact a special function of x, there are limited possibilities to compute it in a closed form. One point where the sum is known is $x=1$, as shown in the following theorem.

Theorem 6: (The sum for $x=1$) Let μ_1, μ_2, ν_1 and ν_2 are nonnegative integer constants. Then

$$\sum_{m=0}^{+\infty} \binom{n-\nu_1}{m-\mu_1}\binom{n-\nu_2}{m-\mu_2} = \binom{2n-(\nu_1+\nu_2)}{n-(\nu_2-\mu_2+\mu_1)}. \tag{B.4}$$

Proof: Without loss of generality, let us assume that $\mu_1 \ge \mu_2$. Using Lemma 5, the sum can then be rewritten to

$$\sum_{m=\mu_1}^{n-\nu_2+\mu_2} \binom{n-\nu_1}{m-\mu_1}\binom{n-\nu_2}{m-\mu_2}. \tag{B.5}$$

By substituting $k = m - \mu_1$, it transforms into

$$\sum_{k=0}^{n-\nu_2+\mu_2-\mu_1} \binom{n-\nu_1}{k} \binom{n-\nu_2}{k+\mu_1-\mu_2}. \tag{B.6}$$

Let us further study the following two expansions given by the binomial theorem:

$$\begin{aligned} (1+x)^{n-\nu_1} &= \sum_{k=0}^{n-\nu_1} \binom{n-\nu_1}{k} x^k, \\ (1+x)^{n-\nu_2} &= \sum_{l=0}^{n-\nu_2} \binom{n-\nu_2}{l} x^l. \end{aligned} \tag{B.7}$$

Their product can be expressed as

$$\begin{aligned} (1+x)^{n-\nu_1}(1+x)^{n-\nu_2} &= \sum_{k=0}^{n-\nu_1} \sum_{l=0}^{n-\nu_2} \binom{n-\nu_1}{k} \binom{n-\nu_2}{l} x^{k+l} = \\ &= \sum_{m=0}^{2n-\nu_1-\nu_2} \sum_{k=0}^{m} \binom{n-\nu_1}{k} \binom{n-\nu_2}{m-k} x^m = \\ &= \sum_{m=0}^{2n-\nu_1-\nu_2} \sum_{k=0}^{m} \binom{n-\nu_1}{k} \binom{n-\nu_2}{k+n-\nu_2-m} x^m. \end{aligned} \tag{B.8 a}$$

However, we could multiply the powers and expand the result:

$$\begin{aligned} (1+x)^{n-\nu_1}(1+x)^{n-\nu_2} &= (1+x)^{2n-\nu_1-\nu_2} = \\ &= \sum_{m=0}^{2n-\nu_1-\nu_2} \binom{2n-\nu_1-\nu_2}{m} x^m. \end{aligned} \tag{B.8 b}$$

Both Eqs. (B.8 a) and (B.8 b) are finite power expansions of the same expression, thus the coefficients of the same power of x must be equal. We can note that the coefficient of x^m, $m = n - \nu_2 + \mu_2 - \mu_1$, in Eq. (B.8 a) is exactly the sum in Eq. (B.6). Therefore, this sum must be equal to the coefficient of x^m in Eq. (B.8 b), which is

$$\binom{2n-\nu_1-\nu_2}{m} = \binom{2n-\nu_1-\nu_2}{n-\nu_2+\mu_2-\mu_1}.$$

■

The following theorem shows that for large n, the sum rises exponentially in n, and it gives the quotient of this grow.

Theorem 7: Let μ_1, μ_2, ν_1 and ν_2 are nonnegative integer constants, let x is real, $x \geq 0$. The limit

$$q(x) = \lim_{n \to +\infty} \sqrt[n]{\sum_{m=0}^{+\infty} \binom{n-\nu_1}{m-\mu_1} \binom{n-\nu_2}{m-\mu_2} x^n} \tag{B.9}$$

exists and equals $(\sqrt{x}+1)^2$.

To prove this theorem, we will first need the following useful lemma:

Lemma 8: Let the assumptions of Theorem 7 hold, let $n \in N$ and x are fixed. Then the expression

$$\binom{n-\nu_1}{m-\mu_1}\binom{n-\nu_2}{m-\mu_2}x^n \tag{B.10}$$

has exactly one maximum in m. For $n \gg \mu_i$, $n \gg \nu_i$, the maximum is reached at

$$m_0 = \frac{\sqrt{x}}{\sqrt{x}+1}n + O(1). \tag{B.11}$$

Proof: Let us denote

$$a_m = \binom{n-\nu_1}{m-\mu_1}\binom{n-\nu_2}{m-\mu_2}x^n. \tag{B.12}$$

Let us study the ratio of two succeeding terms in the interval where they are nonzero, as given by Lemma 5:

$$\frac{a_{m+1}}{a_m} = \frac{(n-\nu_1-m+\mu_1)(n-\nu_2-m+\mu_2)}{(m-\mu_1+1)(m-\mu_2+1)}x. \tag{B.13}$$

This is a rational function in m. In the allowed interval, the denominator is a monotonically increasing function and the numerator a monotonically decreasing function. Depending on the value in the minimal and maximal m given by the inequality (B.2), the sequence (a_m) is either monotonically decreasing, monotonically increasing or has one maximum inside the interval. In all cases, there is exactly one maximum.[2] For sufficiently large n, the maximum is reached inside the interval and can be found putting the ratio (B.13) equal to 1. This leads to a quadratic equation for m, which can be written asymptotically as

$$\begin{aligned}(n^2 - 2mn + m^2 + O(n,m))x &= m^2 + O(m)\\ (x-1)\left(\frac{m}{n}\right)^2 - 2x\left(\frac{m}{n}\right) + x + O(n^{-1}) &= 0.\end{aligned} \tag{B.14}$$

This equation has two asymptotic solutions,

$$\frac{m}{n} = \frac{x \pm \sqrt{x}}{x-1} + O(n^{-1}) = \frac{\sqrt{x}}{\sqrt{x}\mp 1} + O(n^{-1}), \tag{B.15}$$

from which only the + variant is acceptable since the other one gives m outside the bounds (B.2). Multiplying the last equation by n completes the proof. ■

Proof of Theorem 7: Let A_n denote the maximal value of (B.10) for given $n \in N$. We can then estimate the root from both sides by

$$\sqrt[n]{A_n} \le \sqrt[n]{\sum_{m=0}^{+\infty}\binom{n-\nu_1}{m-\mu_1}\binom{n-\nu_2}{m-\mu_2}x^n} \le \sqrt[n]{(n+1)A_n}. \tag{B.16}$$

[2] Under special conditions, it can happen that the same maximal value is reached at two consecutive values of m. We will consider this also a single maximum.

As n approaches $+\infty$, the $\sqrt[n]{n+1}$ term has a limit of 1, so both sides give the same value

$$q(x) = \lim_{n\to+\infty} \sqrt[n]{A_n}. \tag{B.17}$$

We will estimate the maximum A_n using its approximate position given by the above Lemma. Let us denote

$$\alpha = \frac{\sqrt{x}}{\sqrt{x}+1}, \tag{B.18}$$

so that $m_0 = \alpha n + O(1)$.

First, let us use the Stirling's approximation [26]

$$n! = \sqrt{2\pi n}\left(\frac{n}{e}\right)^n \left(1 + O(n^{-1})\right) \tag{B.19}$$

to make a similar approximation of a binomial coefficient, $\binom{n}{k}$, when n is large and both k and $n-k$ are $\Omega(n)$:

$$\binom{n}{k} = \frac{n^{n+\frac{1}{2}}}{\sqrt{2\pi}k^{k+\frac{1}{2}}(n-k)^{n-k+\frac{1}{2}}} \left(1 + O(n^{-1})\right) \tag{B.20}$$

This condition is met for $k = m_0 - \mu_i$ when $\alpha \in (0,1)$.

Using this approximation formula for A_n gives

$$A_n = \frac{(n-\nu_1)^{n-\nu_1+\frac{1}{2}}(n-\nu_2)^{n-\nu_2+\frac{1}{2}}x^{\alpha n}}{2\pi(\alpha n+O)^{\alpha n+O}(\alpha n+O)^{\alpha n+O}(\alpha' n+O)^{\alpha' n+O}(\alpha' n+O)^{\alpha' n+O}} \tag{B.21}$$

where every O is a shorthand for $O(1)$ and

$$\alpha' = 1 - \alpha = \frac{1}{\sqrt{x}+1}. \tag{B.22}$$

We can use this estimate to finally compute the limit (B.17). In the following, $O' \equiv O(n^{-1})$.

$$\begin{aligned} q(x) &= \lim_{n\to+\infty} \sqrt[n]{A_n} = \\ &= \lim_{n\to+\infty} \sqrt[n]{\frac{(n-\nu_1)^{n-\nu_1+\frac{1}{2}}(n-\nu_2)^{n-\nu_2+\frac{1}{2}}x^{\alpha n}}{2\pi(\alpha n+O)^{\alpha n+O}(\alpha n+O)^{\alpha n+O}(\alpha' n+O)^{\alpha' n+O}(\alpha' n+O)^{\alpha' n+O}}} = \\ &= \lim_{n\to+\infty} \frac{(n-\nu_1)^{1+O'}(n-\nu_2)^{n+O'}x^{\alpha}}{(2\pi)^{\frac{1}{n}}(\alpha n+O)^{\alpha+O'}(\alpha n+O)^{\alpha+O'}(\alpha' n+O)^{\alpha'+O'}(\alpha' n+O)^{\alpha'+O'}} \end{aligned} \tag{B.23 a}$$

After this step, the O' terms in all the exponents can be dropped as a result of $\Theta(n)^{O(1/n)} \to 1$. Similarly, the $(2\pi)^{1/n}$ term has a limit of 1:

$$\begin{aligned} q(x) &= \lim_{n\to+\infty} \frac{(n-\nu_1)(n-\nu_2)x^{\alpha}}{(\alpha n+O)^{\alpha}(\alpha n+O)^{\alpha}(\alpha' n+O)^{\alpha'}(\alpha' n+O)^{\alpha'}} = \\ &= \lim_{n\to+\infty} \frac{(1-\frac{\nu_1}{n})(1-\frac{\nu_2}{n})x^{\alpha}}{(\alpha+O')^{\alpha}(\alpha+O')^{\alpha}(\alpha'+O')^{\alpha'}(\alpha'+O')^{\alpha'}} \end{aligned} \tag{B.23 b}$$

In the first line of Eq. (B.23 b), we divided both sides of the fraction by n^2, using the fact that $2(\alpha + \alpha') = 2$. As α and α' are constant, we can take the limit easily:

$$\begin{aligned} q(x) &= \frac{x^{\alpha}}{\alpha^{\alpha}\alpha^{\alpha}{\alpha'}^{\alpha'}(\alpha')^{\alpha'}} \\ &= \frac{x^{\alpha}}{\alpha^{2\alpha}{\alpha'}^{2\alpha'}} \\ &= \frac{x^{\frac{\sqrt{x}}{\sqrt{x}+1}}}{\left(\frac{\sqrt{x}}{\sqrt{x}+1}\right)^{2\frac{\sqrt{x}}{\sqrt{x}+1}}\left(\frac{1}{\sqrt{x}+1}\right)^{2\frac{1}{\sqrt{x}+1}}} \\ &= (\sqrt{x}+1)^2. \end{aligned} \tag{B.23 c}$$

■

Bibliography

[1] Travaglione, B. C., Milburn G. J. *Implementing the quantum random walk.* Phys. Rev. A, **65**, 032310 (2002)

[2] Zhao, Z. et al. *Implement Quantum Random Walks with Linear Optics Elements.* arXiv:quant-ph/0212149v1

[3] Du, J. et al. *Experimental implementation of the quantum random-walk algorithm.* Phys. Rev. A, **67**, 042316 (2003)

[4] Schreiber, A., Cassemiro, K., Silberhorn, C. DPG poster presentation (2009), more results to be published

[5] Aharonov, Y., Davidovich, L., Zagury, N. *Quantum random walks.* Phys. Rev. A, **48**, pp. 1687–1690 (1993)

[6] Nayak, A., Vishwanath, A. *Quantum walk on the line.* arXiv:quant-ph/0010117

[7] Ambainis, A. *Quantum walks and their algorithmic applications.* Int. J. Quantum Info, **1**, pp. 507-518 (2003)

[8] Kempe, J. *Quantum random walks – an introductory overview.* Cont. Phys., **44** (4), pp. 307–327 (2003)

[9] Meyer, D. A. *On the absence of homogenous scalar unitary cellular automata.* arXiv:quant-ph/ /9604011v2

[10] Ambainis, A., Kempe, J., Rivosh, A. *Coins Make Quantum Walks Faster.* arXiv:quant-ph/ /0402107

[11] Kempe, J. *Quantum Random Walks Hit Exponentially Faster.* arXiv:quant-ph/0205083

[12] Aharonov, D., Ambainis, A., Kempe, J., Vazirani, U. *Quantum walks on graphs.* arXiv:quant-ph/0012090v2

[13] Shenvi, N., Kempe, J., Whaley, K. *Quantum Random Walk Search Algorithm.* Phys. Rev. A, **67**, 052307 (2003)

[14] Farhi, E., Gutmann, S. *Quantum computation and decision trees.* Phys. Rev. A, **58**, 915 (1998)

[15] Childs, A. M. et al. *Exponential algorithmic speedup by quantum walk.* arXiv:quant-ph/ /0209131v2

[16] Childs, A. M. *On the relationship between continuous- and discrete-time quantum walk.* arXiv: :0810.0312v2 [quant-ph]

[17] D'Alessandro, D. *Connection Between Continuous and Discrete Time Quantum Walks on d-Dimensional Lattices; Extensions to General Graphs.* arXiv:0902.3496v1 [quant-ph]

[18] Bachor, H. A., Ralph, T. C. *A Guide to Experiments in Quantum Optics, 2^{nd} ed.* Wiley-VCH, Berlin, Germany

[19] Silberhorn, C. *Detecting quantum light.* Cont. Phys., **48** (3), pp. 143–156 (2007)

[20] Schleich, W. P. *Quantum Optics in Phase Space.* Wiley-VCH, Berlin, Germany

[21] Petkovšek, M., Wilf, H. S., Zeilberger, D. *A=B*. A K Peters, Wellesley, USA, 1996

[22] Erdélyi, A. et al. *Higher Transcendental Functions, Vol. 1.* Krieger, New York, USA, 1981

[23] Koepf, W. *Hypergeometric Summation: An Algorithmic Approach to Summation and Special Function Identities.* Braunschweig, Wiesbaden, Germany (1998)

[24] Abramowitz, M., Stegun, I. A. (Eds.) *Handbook of Mathematical Functions with Formulas, Graphs, and Mathematical Tables, 9^{th} printing.* Dover, New York, USA, 1972

[25] Tweddle, I. *James Stirling's Methodus Differentialis: An Annotated Translation of Stirling's Text.* Springer, London, UK, 2003

[26] Weisstein, E. W. *Stirling's Approximation.* From MathWorld—A Wolfram Web Resource. <http://http://mathworld.wolfram.com/StirlingsApproximation.html> [Accesed 28 Apr 2009]

[27] Scully, M. O., Zubairy, M. S. *Quantum optics.* Cambridge University Press, Cambridge, UK, 1997

[28] Nielsen, M. A., Chuang, I. L. *Quantum Computation and Quantum Information.* Cambridge University Press, Cambridge, UK, 2000

[29] Kendon, V. *Decoherence in quantum walks – a review.* arXiv:quant-ph/0606016v3

[30] Born, M., Wolf, E. *Principles of Optics, 7^{th} ed.* Cambridge University Press, Cambridge, UK, 1999

[31] Griffiths, D. J. *Introduction to Quantum Mechanics, 2^{nd} ed.* Pearson Prentice Hall, Upper Saddle River, USA, 2005

Prohlášení

Prohlašuji, že jsem svou diplomovou práci vypracoval samostatně a použil jsem pouze literaturu uvedenou v přiloženém seznamu.

Nemám závažný důvod proti užití tohoto školního díla ve smyslu § 60 Zákona č. 121/2000 Sb., o právu autorském, o právech souvisejících s právem autorským a o změně některých zákonů (autorský zákon).

V Praze dne ....
podpis